Electronic Supplementary Material (ESI) for Physical Chemistry Chemical Physics.
This journal is © the Owner Societies 2022

The Binding Mechanism of NHWD-870 to Bromodomain Containing Protein 4 Based on Molecular Dynamics Simulations and Free Energy Calculation

Mingsong Shi[a], Jun He[a], Tiantian Weng[a], Na Shi[a], Wenyan Qi[a], Yong Guo[a], Tao Chen[a], Lijuan Chen[a]* and Dingguo Xu[b,c]*

[a]State Key Laboratory of Biotherapy/Collaborative Innovation Center of Biotherapy and Cancer Center, West China Hospital of Sichuan University, Chengdu, Sichuan 610041, China

[b]College of Chemistry, MOE Key Laboratory of Green Chemistry and Technology, Sichuan University, Chengdu, Sichuan 610064, China

[c]Research Center for Material Genome Engineering, Sichuan University, Chengdu, Sichuan 610065, China

***Corresponding authors:** dgxu@scu.edu.cn (D. X.), +86-13551230257; chenlijuan125@163.com (L. C.), +86-18980601790.

Contents

Method for Binding Free Energy Estimation

In this work, the molecular mechanics generalized Born surface area (MM/GBSA) approach[1, 2] were employed to calculate the binding free energies of NHWD-870 to BRD4 (BD1 and BD2). It is an efficient method to improve the ability evaluation of ligand and protein systems[3-5]. The MM/GBSA framework has been discussed extensively[6-8]. Only a short description is summarized here. The total binding free energy for the binding of NHWD-870 of BRD4-BD1 and BRD4-BD2, namely $\Delta G_{binding}$ was provide in the following:

$$\Delta G_{binding} = \Delta G_{complex} - \Delta G_{protein} - \Delta G_{ligand} \quad (1)$$

$$G = E_{gas} + G_{sol} - TS \quad (2)$$

$$E_{gas} = E_{int} + E_{vdW} + E_{ele} \quad (3)$$

$$G_{sol} = G_{el} + G_{nonel} \quad (4)$$

$\Delta G_{complex}$, $\Delta G_{protein}$ and ΔG_{ligand} are denoted as free energies of the NHWD-870/BD1 or BD2 of BRD4, BD1 or BD2 of BRD4 and NHWD-870, respectively. The $\Delta G_{binding}$ can be decomposed into the enthalpy part ($\Delta H = E_{gas} + G_{sol}$) and the entropy part ($T\Delta S$). The molecular mechanical energies (E_{gas}) consist of the intramolecular energy (E_{int}), van der Waals forces (E_{vdW}) and electrostatic forces (E_{ele}) which get these values via a statistical average way based on the AMBER force field. The solvation free energy (G_{sol}) can be principally divided into both electrostatic (G_{el}) and non-electrostatic (G_{nonel}) terms. The G_{nonel} comes from the combined effect of unfavorable cost of surface formation and the favorable van der Waals interactions between the solute and solvent, which can be evaluated by the equation of $\gamma \cdot SA + b$, where γ =0.0072 kcal/Å^2 and b=0.0 kcal/mol. The solvent accessible surface area (SA) which was estimated using the LCPO method[9]. The G_{el} is calculated by the Generalized Born (GB) equation[10, 11]. The solute dielectric constant was set to 1, and the exterior dielectric constant was set to 80. We used MM/GBSA method to get these former terms via a statistical average way from the last 200 ns MD trajectory. Meanwhile, entropy contributions to the binding free energy may be added to improve the accuracy. The entropy can be estimated using the normal model analysis with quasi harmonic model based on the conformational snapshots from the same MD trajectory[12]. For each complex system, binding energies were averaged over 1000 frames and the -TS was averaged with interval 2 ns. Those energy was calculated with the MMPBA.py program[13].

Method for HTRF Assay

Recombinant protein BRD4(D1) (RBC, Cat. No. RD-11-157), BRD2(D2) (Active Motif, Cat. No. 31378), and compound (+)-JQ1 (BPS, Cat. No. 27402) were obtained from Shanghai ChemPartner Co., Ltd. NHWD-870 (Cat. No. HY-134463) was purchased from MedChem Express. The compounds were serially diluted in Echo plate according to the plate map. The DMSO final fraction was 0.1%. The compound/DMSO was transferred to a 384-well assay plate (384-well OptiPlate (Perkin Elmer, Cat. No. 6007299)) by Echo, followed by the addition of the 2x protein and peptide mix to the assay plate. Subsequently, the 2x detection mix was added to the assay plate with shaking for 30 seconds. The plate was incubated at 25 ℃for 1 hour. The HTRF signals (Ex at 340nm, Em at 615nm & 665 nm) were read using EnVision. The data was fed into Excel to obtain the inhibition values using equation (1): inh %=(Max-Signal)/ (Max-Min)*100. The data was fit in XL-Fit to obtain IC_{50} values using equation (2): Y=Bottom + (Top-Bottom)/(1+(IC50/X)*HillSlope). Y is the %inhibition and X is the compound concentration.

Reference

1. Srinivasan, J.; Cheatham, T. E.; Cieplak, P.; Kollman, P. A.; Case, D. A., Continuum solvent studies of the stability of DNA, RNA, and phosphoramidate - DNA helices. *J. Am. Chem. Soc.* **1998,** *120* (37), 9401-9409.
2. Lee, M. S.; Salsbury, F. R.; Olson, M. A., An efficient hybrid explicit/implicit solvent method for biomolecular simulations. *J. Comput. Chem.* **2004,** *25* (16), 1967-1978.
3. Shi, M.; Xu, D., Molecular dynamics investigations suggest a non-specific recognition strategy of 14-3-3σ protein by tweezer: Implication for the inhibition mechanism. *Front. Chem.* **2019,** *7* (237).
4. Wang, J. Y.; Chen, Q.; Wang, M.; Zhong, C., The opening/closure of the P-loop and hinge of BCR-ABL1 decodes the low/high bioactivities of dasatinib and axitinib. *Phys. Chem. Chem. Phys.* **2017,** *19* (33), 22444-22453.
5. Tse, A.; Verkhivker, G. M., Molecular Dynamics Simulations and Structural Network Analysis of c-Abl and c-Src Kinase Core Proteins: Capturing Allosteric Mechanisms and Communication Pathways from Residue Centrality. *J. Chem. Inf. Model.* **2015,** *55* (8), 1645-1662.
6. Honig, B.; Nicholls, A., Classical electrostatics in biology and chemistry. *Science* **1995,** *268* (5214), 1144-1149.
7. Genheden, S.; Ryde, U., The MM/PBSA and MM/GBSA methods to estimate ligand-binding affinities. *Expert. Opin. Drug Discov.* **2015,** *10* (5), 449-461.

8. Onufriev, A. V.; Case, D. A., Generalized Born Implicit Solvent Models for Biomolecules. In *Annual Review of Biophysics, Vol 48*, Dill, K. A., Ed. Annual Reviews: Palo Alto, 2019; Vol. 48, pp 275-296.
9. Weiser, J.; Shenkin, P. S.; Still, W. C., Approximate atomic surfaces from linear combinations of pairwise overlaps (LCPO). *J. Comput. Chem.* **1999,** *20* (2), 217-230.
10. Still, W. C.; Tempczyk, A.; Hawley, R. C.; Hendrickson, T., Semianalytical treatment of solvation for molecular mechanics and dynamics. *J. Am. Chem. Soc.* **1990,** *112* (16), 6127-6129.
11. Srinivasan, J.; Trevathan, M. W.; Beroza, P.; Case, D. A., Application of a pairwise generalized Born model to proteins and nucleic acids: inclusion of salt effects. *Theor. Chem. Acc.* **1999,** *101* (6), 426-434.
12. Gao, P. C.; Li, Z. L., Computation of the Boltzmann entropy of a landscape: a review and a generalization. *Landsc. Ecol.* **2019,** *34* (9), 2183-2196.
13. Miller, B. R.; McGee, T. D.; Swails, J. M.; Homeyer, N.; Gohlke, H.; Roitberg, A. E., MMPBSA.py: An Efficient Program for End-State Free Energy Calculations. *Journal of Chemical Theory and Computation* **2012,** *8* (9), 3314-3321.

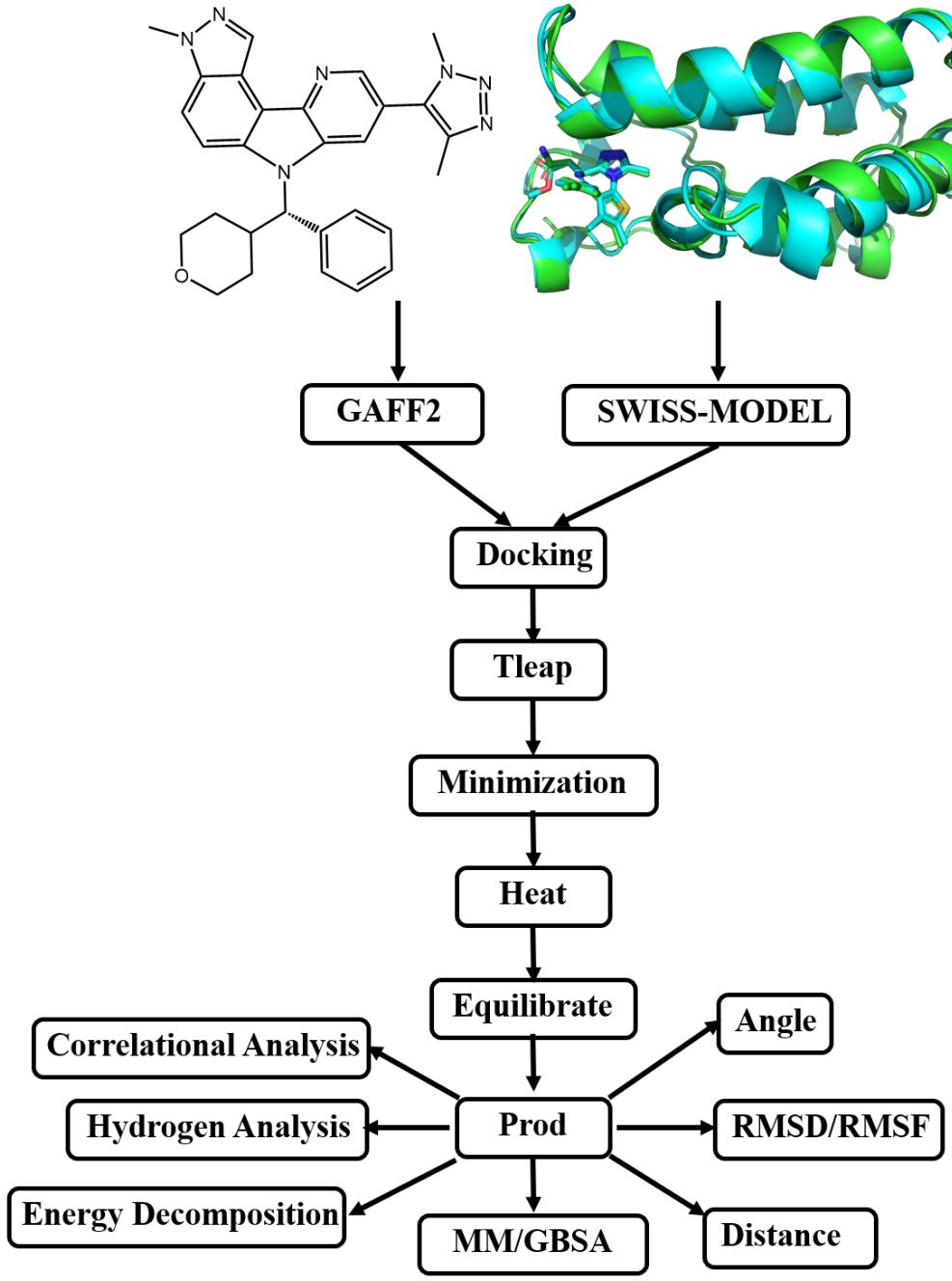

Scheme S1. The methods used in this work.

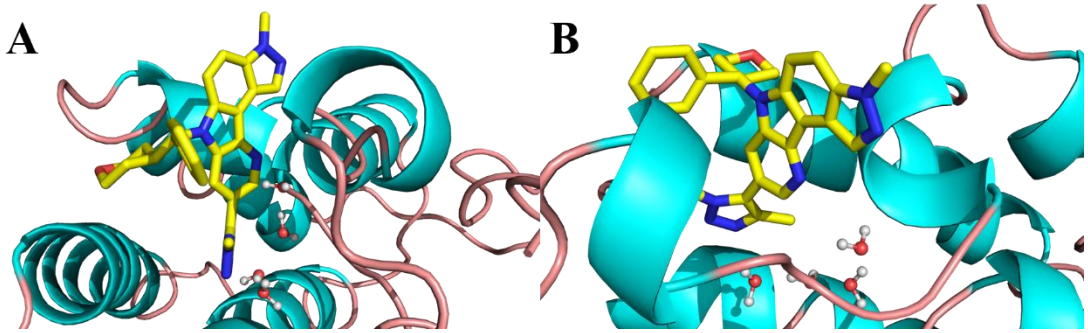

Figure S1. Docking results for NHWD-870 with BRD4-BD1 (A) and translation (B).

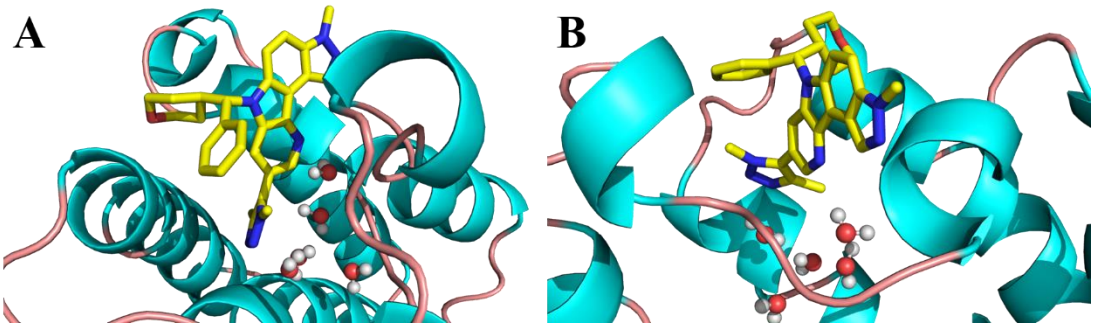

Figure S2. Docking results for NHWD-870 with BRD4-BD2 (A) and translation (B).

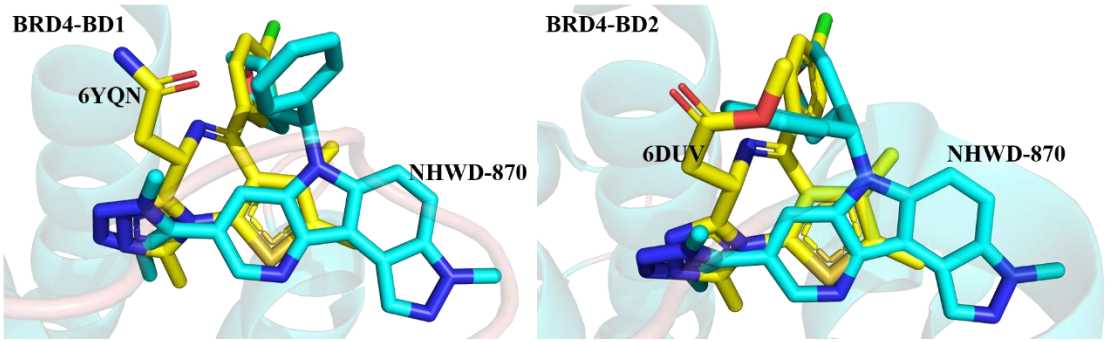

Figure S3. The selected structures from docking and crystal complex structures.

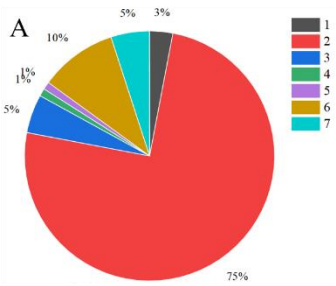

B

Cluster Rank	Lowest Binding Energy	Mean Binding Energy	Number in Cluster	Percentage
	kcal/mol	kcal/mol		%
1	-9.39	-9.21	3	3
2	-9.37	-9.1	75	75
3	-8.19	-8.11	5	5
4	-8.17	-8.17	1	1
5	-8.15	-8.15	1	1
6	-8.13	-7.99	10	10
7	-7.98	-7.96	5	5

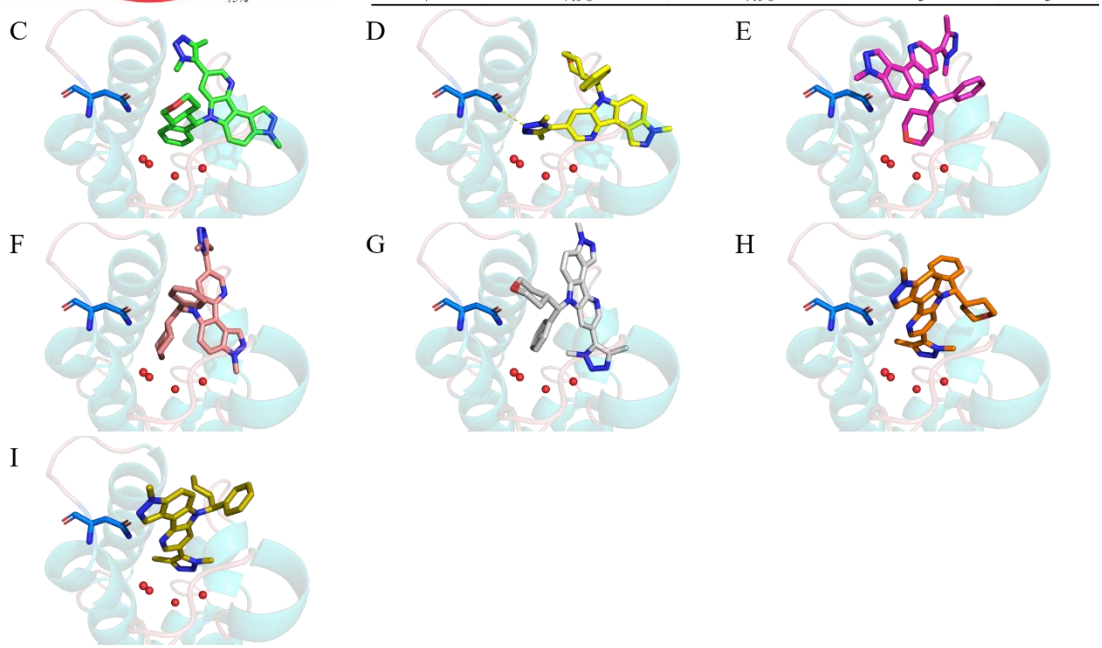

Figure S4. The docking result for NHWD-870 with BRD4-BD1.

(A) for the cluster analysis for the docking 100 conformations. (B) for the detail information for cluster analysis. The representative conformation of NHWD-870 with the lowest energy in the cluster: (C) for cluster 1, (D) for cluster 2, (E) for cluster 3, (F) for cluster 4, (G) for cluster 5, (H) for cluster 6, and (I) for cluster 7. The BRD4-BD1 shown with cartoon, and NHWD-870 with stick. Lowest binding energy is the lowest energy formation in the same cluster; mean binding energy is the mean binding energy for all the conformations in the same cluster; Number in cluster is the conformation number which is located in this cluster; percentage is the percentage for the number in cluster with the total 100 conformations in this docking research.

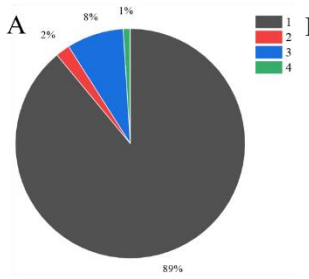

B

Cluster Rank	Lowest Binding Energy	Mean Binding Energy	Number in Cluster	Percentage
	kcal/mol	kcal/mol		%
1	-9.45	-9.17	89	89
2	-9.21	-9.21	2	2
3	-8.89	-8.86	8	8
4	-8.76	-8.76	1	1

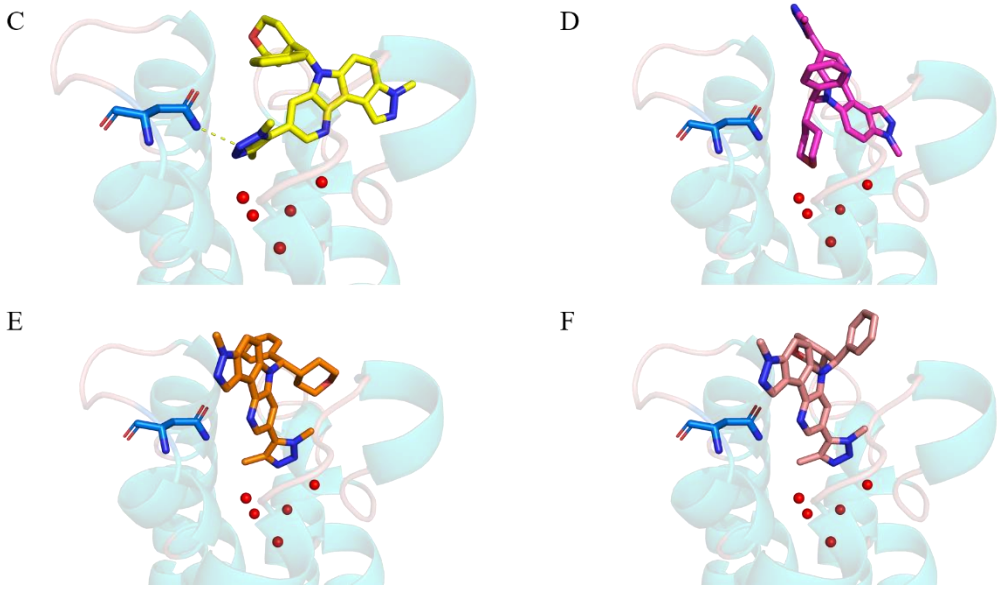

Figure S5. The docking result for NHWD-870 with BRD4-BD2.

(A) for the cluster analysis for the docking 100 conformations. (B) for the detail information for cluster analysis. The representative conformation of NHWD-870 with the lowest energy in the cluster: (C) for cluster 1, (D) for cluster 2, (E) for cluster 3, and (F) for cluster 4. The BRD4-BD2 shown with cartoon, and NHWD-870 with stick. Lowest binding energy is the lowest energy formation in the same cluster; mean binding energy is the mean binding energy for all the conformations in the same cluster; Number in cluster is the conformation number which is located in this cluster; percentage is the percentage for the number in cluster with the total 100 conformations in this docking research.

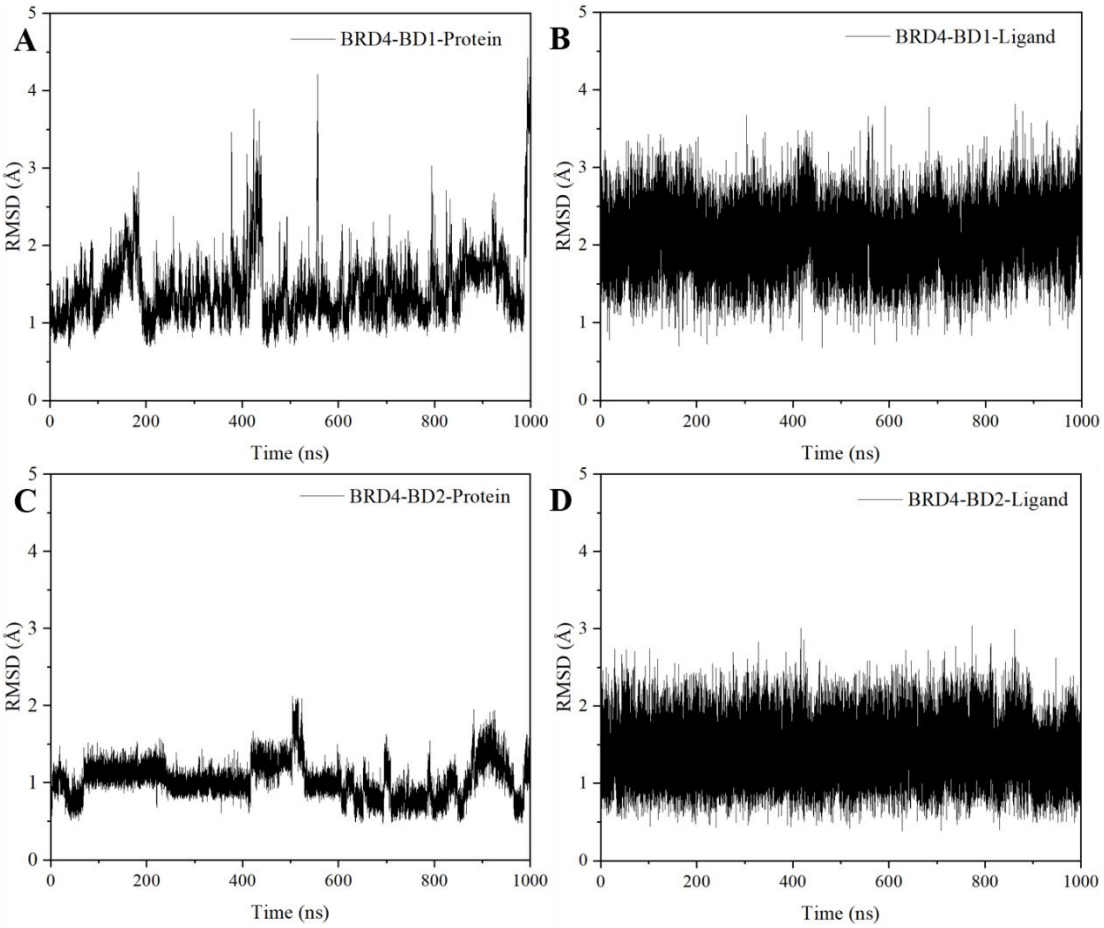

Figure S6. The root mean square deviation (RMSD) value of heavy atoms of backbone of protein and heavy atoms of inhibitor along 1000 ns MD simulations for NHWD-870 with BRD4-BD1 and BD2.

(A) for protein of BRD4-BD1; (B) for inhibitor of BRD4-BD1; (C) for protein of BRD4-BD2; (D) for inhibitor of BRD4-BD2.

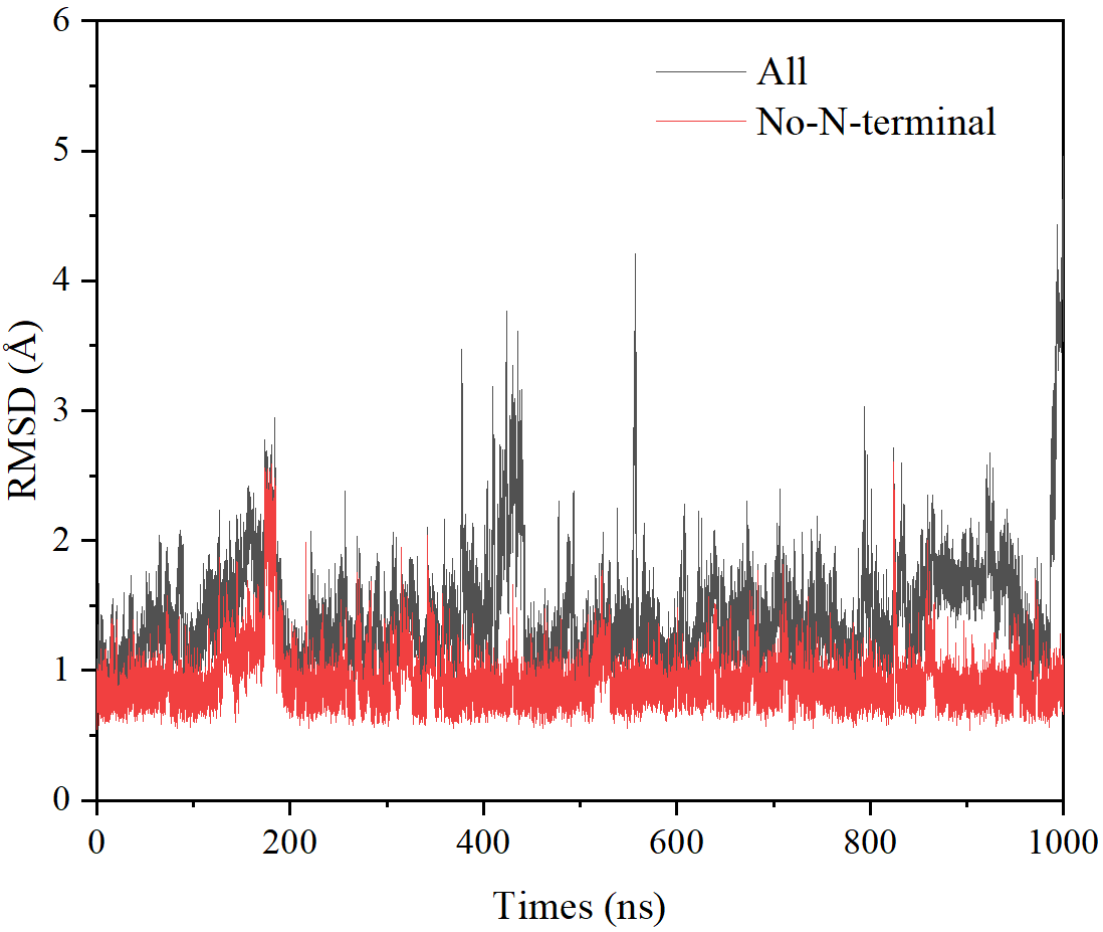

Figure S7. The root mean square deviation (RMSD) value of heavy atoms of backbone of protein along 1000 ns MD simulations for NHWD-870 with BRD4-BD1.

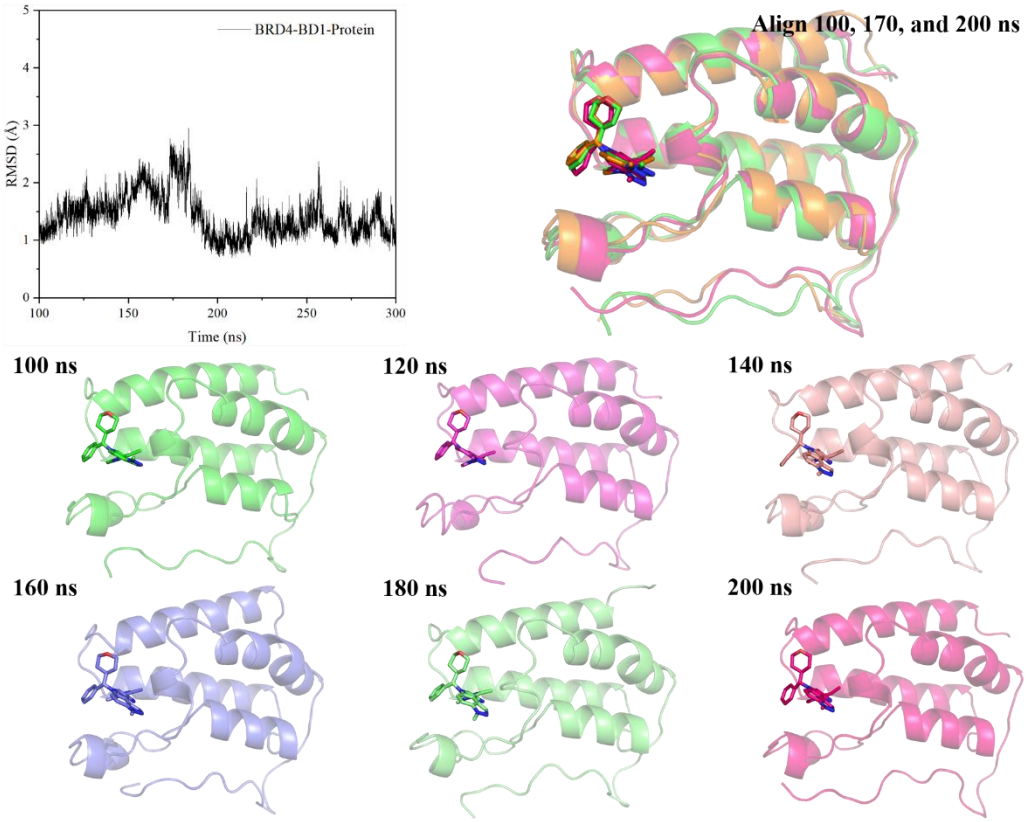

Figure S8. The structures for NHWD-870/BRD4-BD1 with 100-200 ns from MD simulation.

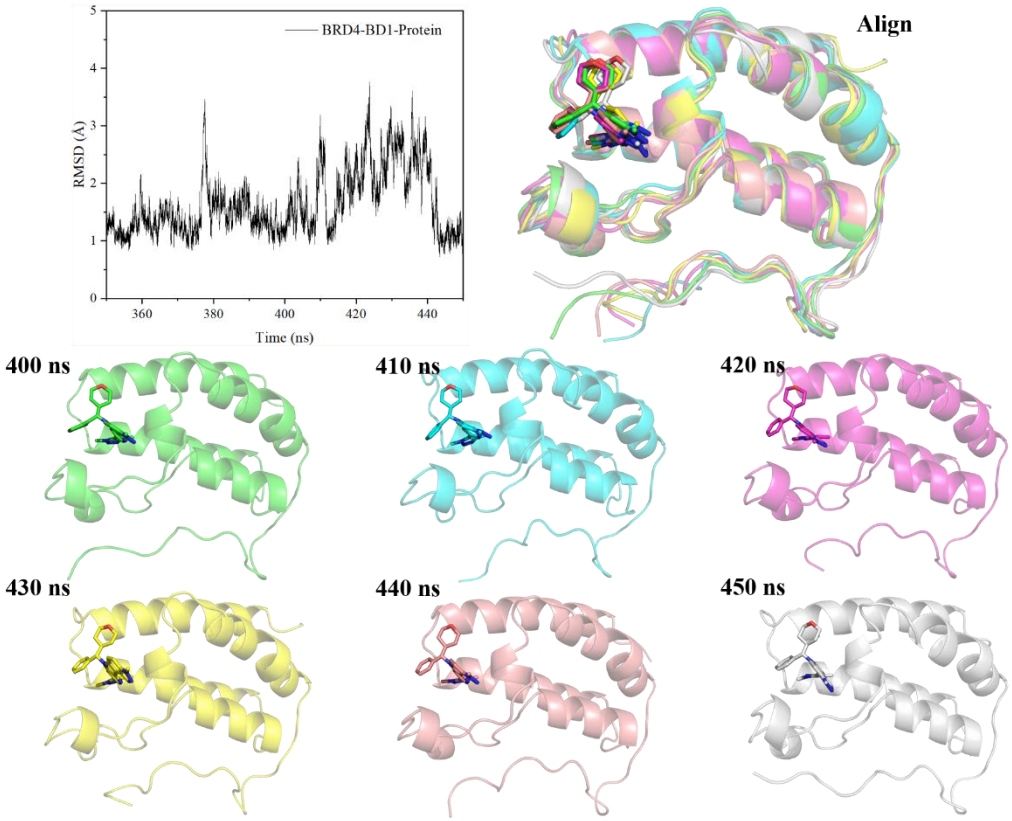

Figure S9. The structures for NHWD-870/BRD4-BD1 with 400-450 ns from MD simulation.

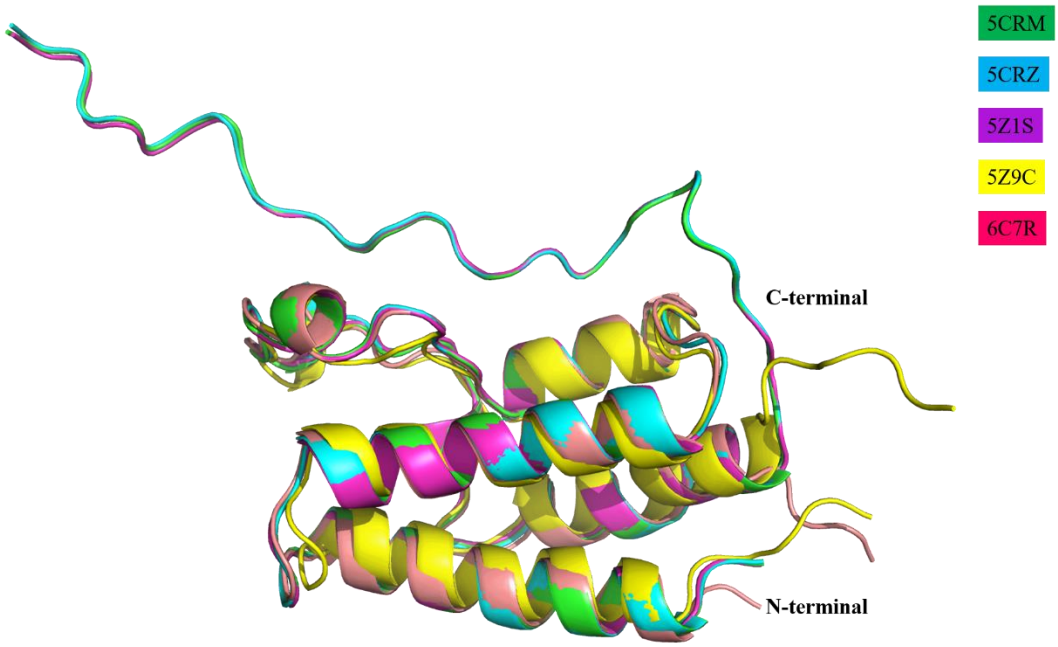

Figure S10. The structures for BRD4-BD1 with different C-terminal tails.

5CRM: 10.1021/acs.jmedchem.5b01511

5CRZ: 10.1021/acs.jmedchem.5b01511

5Z1S: 10.1021/acsmedchemlett.8b00003

5Z9C: 10.1128/JVI.02056-17

6C7R: 10.1021/acs.jmedchem.8b00483

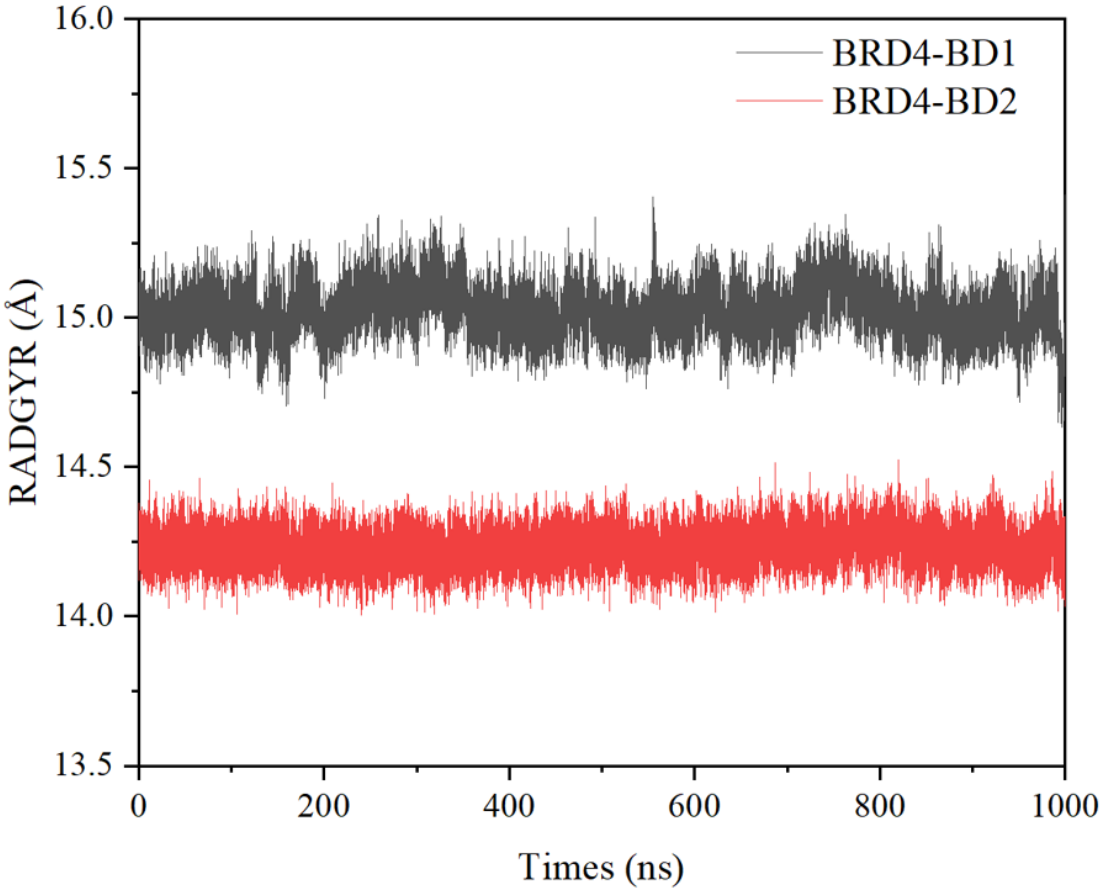

Figure S11. The gyration radius (RADGYR) of NHWD-870 with BRD4-BD1 and BD2.

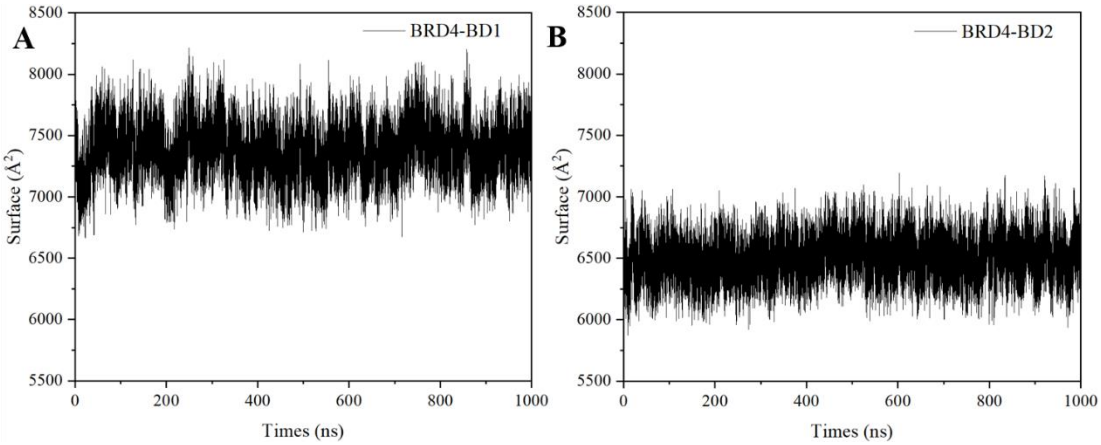

Figure S12. The surface of NHWD-870 with BRD4-BD1 (A) and BD2 (B).

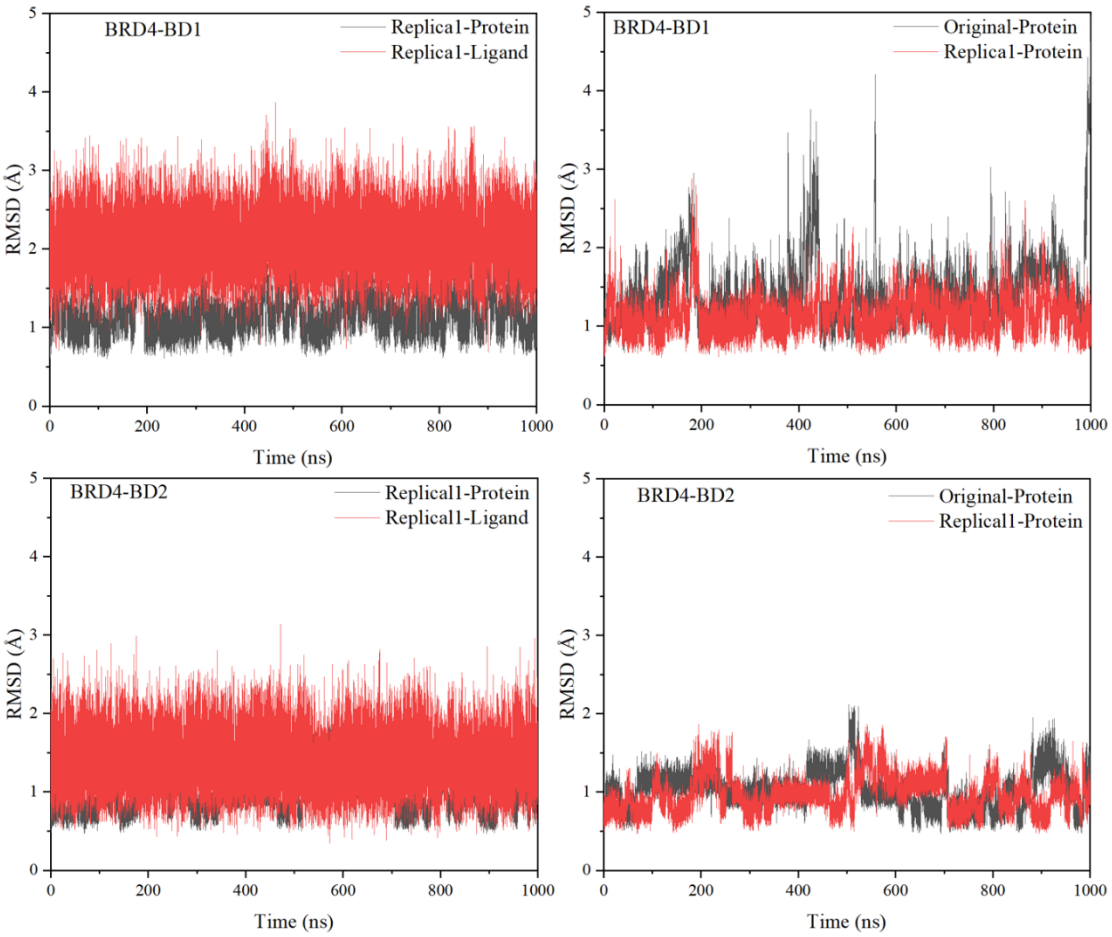

Figure S13. The root mean square deviation (RMSD) value of heavy atoms of backbone of protein and heavy atoms of inhibitor along 1000 ns MD simulations for NHWD-870 with BRD4-BD1 and BD2 from the original simulations and replica simulations.

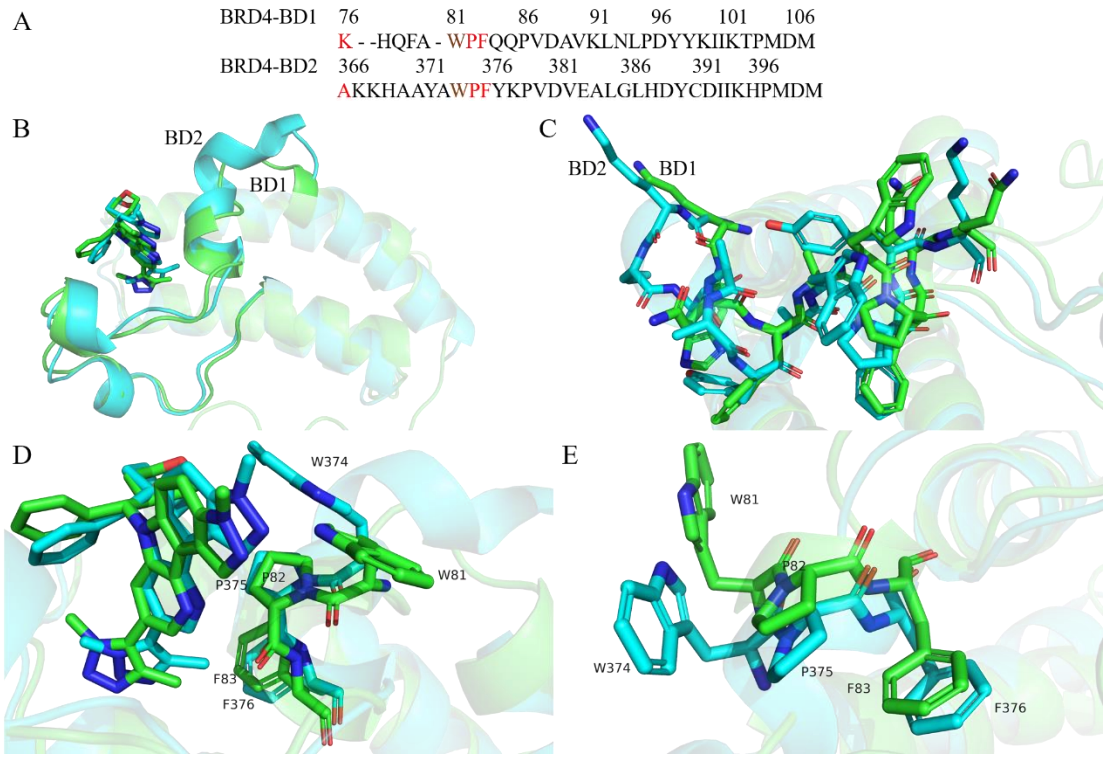

Figure S14. The BC-loop fluctuation of BRD4 in the simulations.

(A) The sequence alignment of BC-loop based on sequence and structure between the BRD4-BD1 and BRD4-BD2. The residues of BC-loop are 76-107 for BRD4-BD1 and 366-400. The residue number is according with human BRD4 protein sequence (UniProt ID: O60885). (B) The structure of BC-loop of BRD4-BD1 and BRD4-BD2 with the NHWD-870. (C) The 76-83 and 366-376 show with stick. (D) The structure of WPF region of BRD4. (E) The other orientation view of the structure of WPF region of BRD4. The green color is used for BRD4-BD1 and cyan for BRD4-BD2. The protein shows with cartoon and NHWD-870 with sticks. The WPF residues shows with sticks. The representative structures were obtained from the cluster analyses of the last 200 ns molecular dynamics simulations for NHWD-870/BRD4-BD1 or NHWD-870/BRD4-BD2 system.

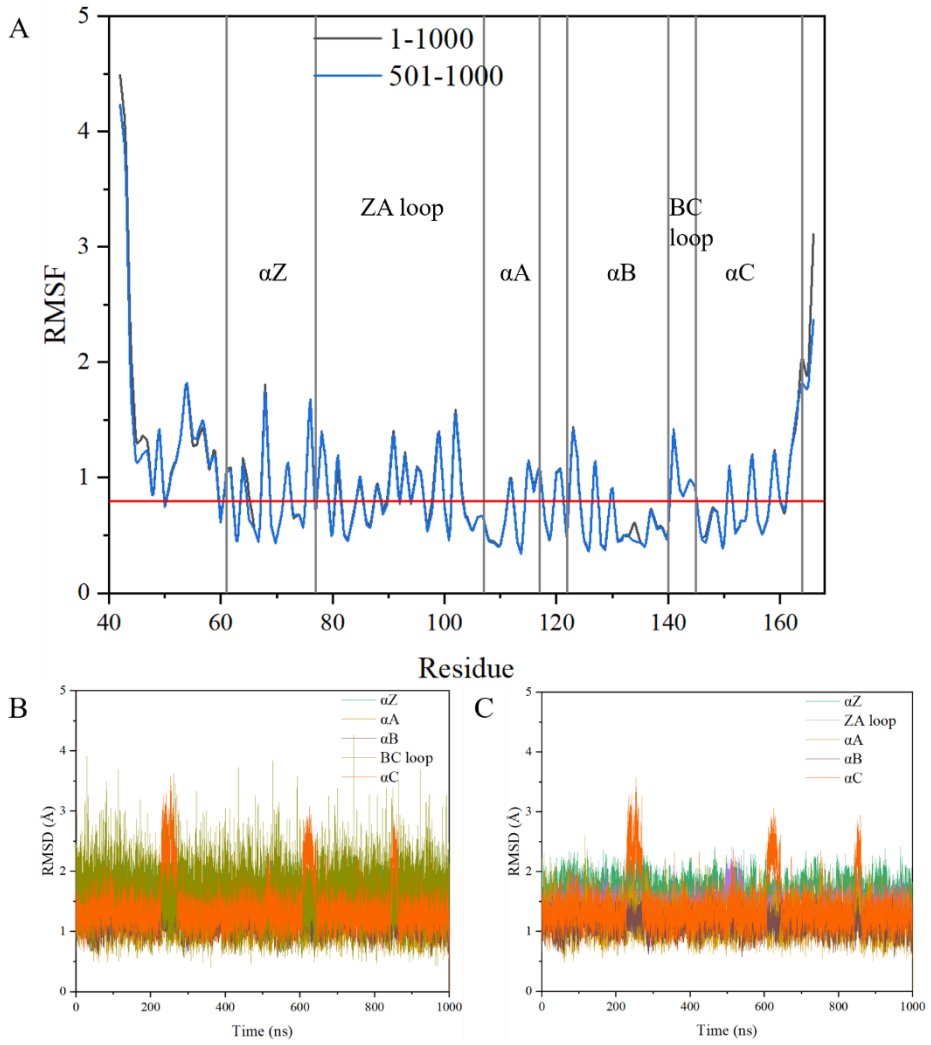

Figure S15. Root mean-squared fluctuation (RMSF) values and root mean square deviation (RMSD) value of BRD4-BD1.

(A) Root mean-squared fluctuation (RMSF) values of the heavy atoms of backbone of all the residues for BRD4-BD1 among the 1000 ns or last 500 ns molecular dynamics simulation. (B) Root mean square deviation (RMSD) value of non-hydrogen atoms of BC-loop calculated among the 1000 ns molecular dynamics simulation as reference with the 1000th conformation and compared with helix domains. (C) Root mean square deviation (RMSD) value of non-hydrogen atoms of ZA-loop calculated among the 1000 ns molecular dynamics simulation as reference with the 1000th conformation and compared with helix domains.

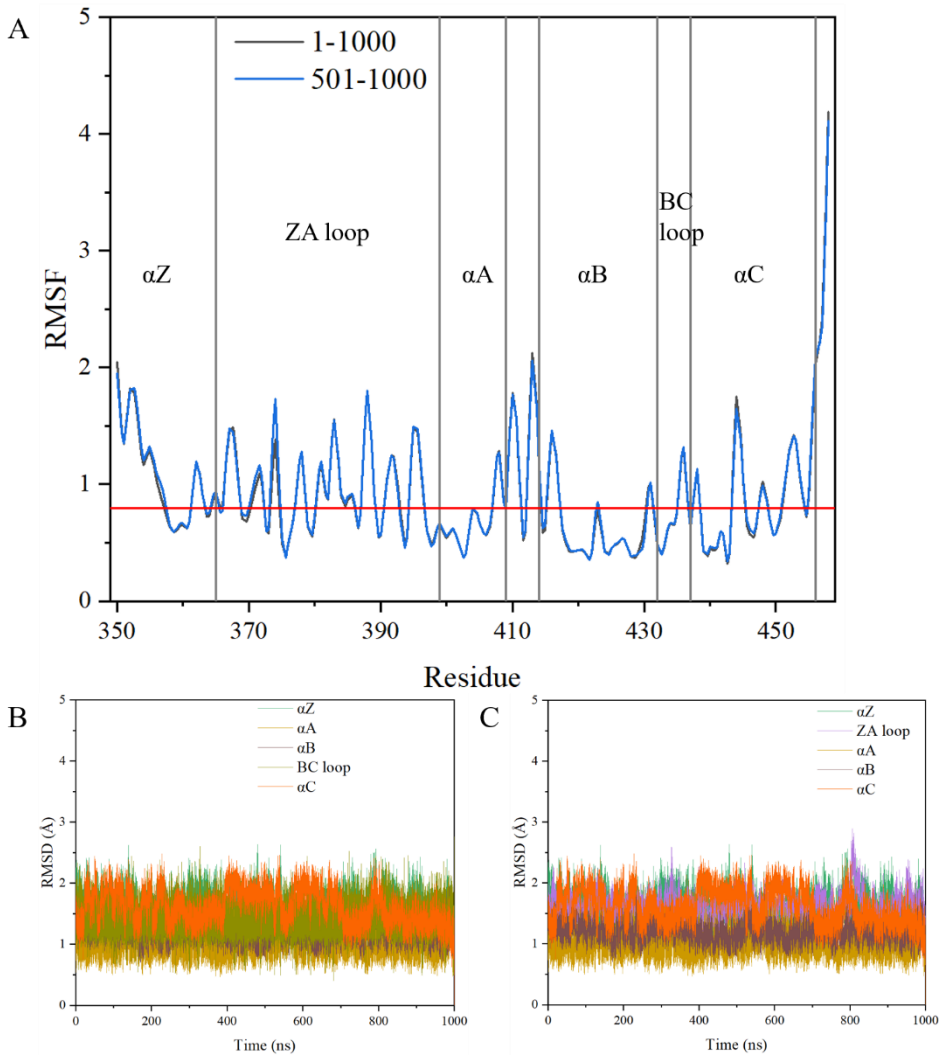

Figure S16. Root mean-squared fluctuation (RMSF) values and root mean square deviation (RMSD) value of BRD4-BD2.

(A) Root mean-squared fluctuation (RMSF) values of the heavy atoms of backbone of all the residues for BRD4-BD2 among the 1000 ns or last 500 ns molecular dynamics simulation. (B) Root mean square deviation (RMSD) value of non-hydrogen atoms of BC-loop calculated among the 1000 ns molecular dynamics simulation as reference with the 1000th conformation and compared with helix domains. (C) Root mean square deviation (RMSD) value of non-hydrogen atoms of ZA-loop calculated among the 1000 ns molecular dynamics simulation as reference with the 1000th conformation and compared with helix domains.

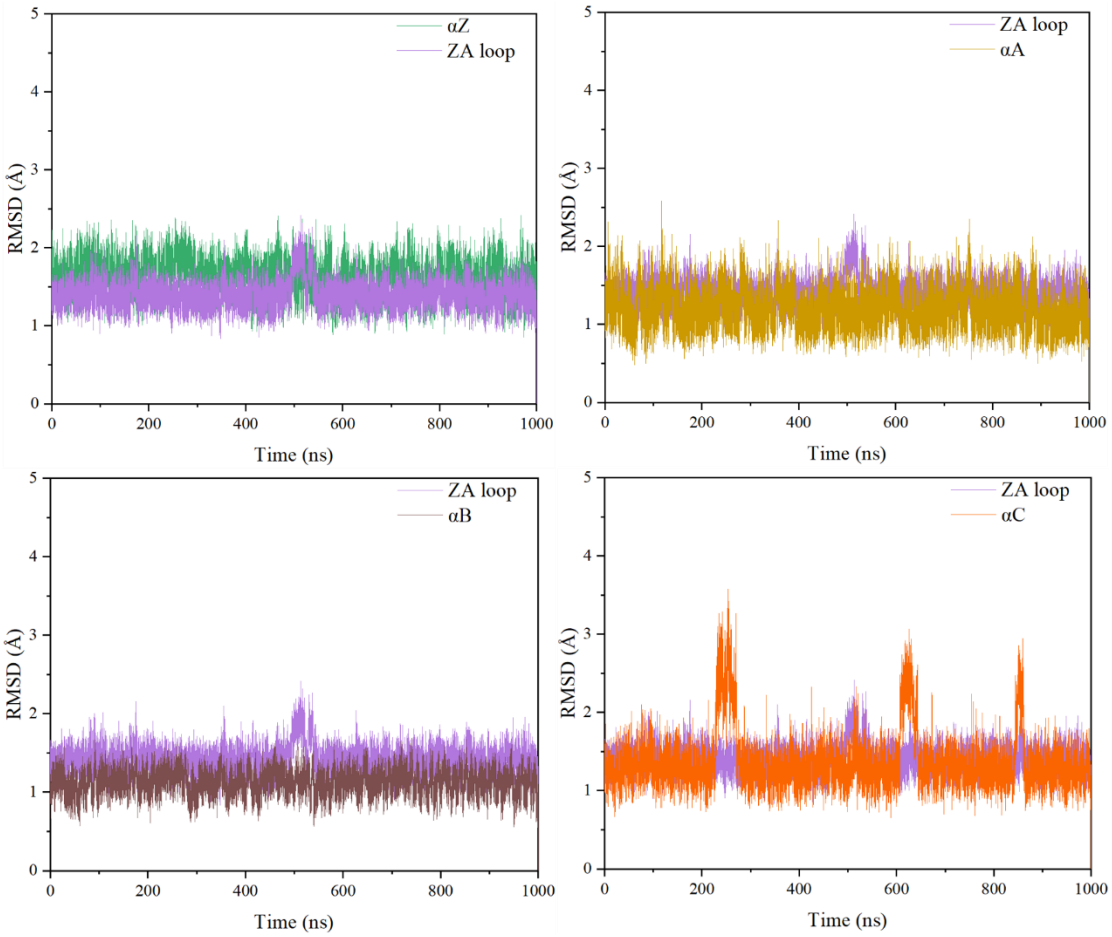

Figure S17. Root mean square deviation (RMSD) value of ZA-loop compared with helices of BRD4-BD1.

Root mean square deviation (RMSD) value of non-hydrogen atoms of ZA-loop calculated among the 1000 ns molecular dynamics simulation as reference with the 1000th conformation and compared with helix domains.

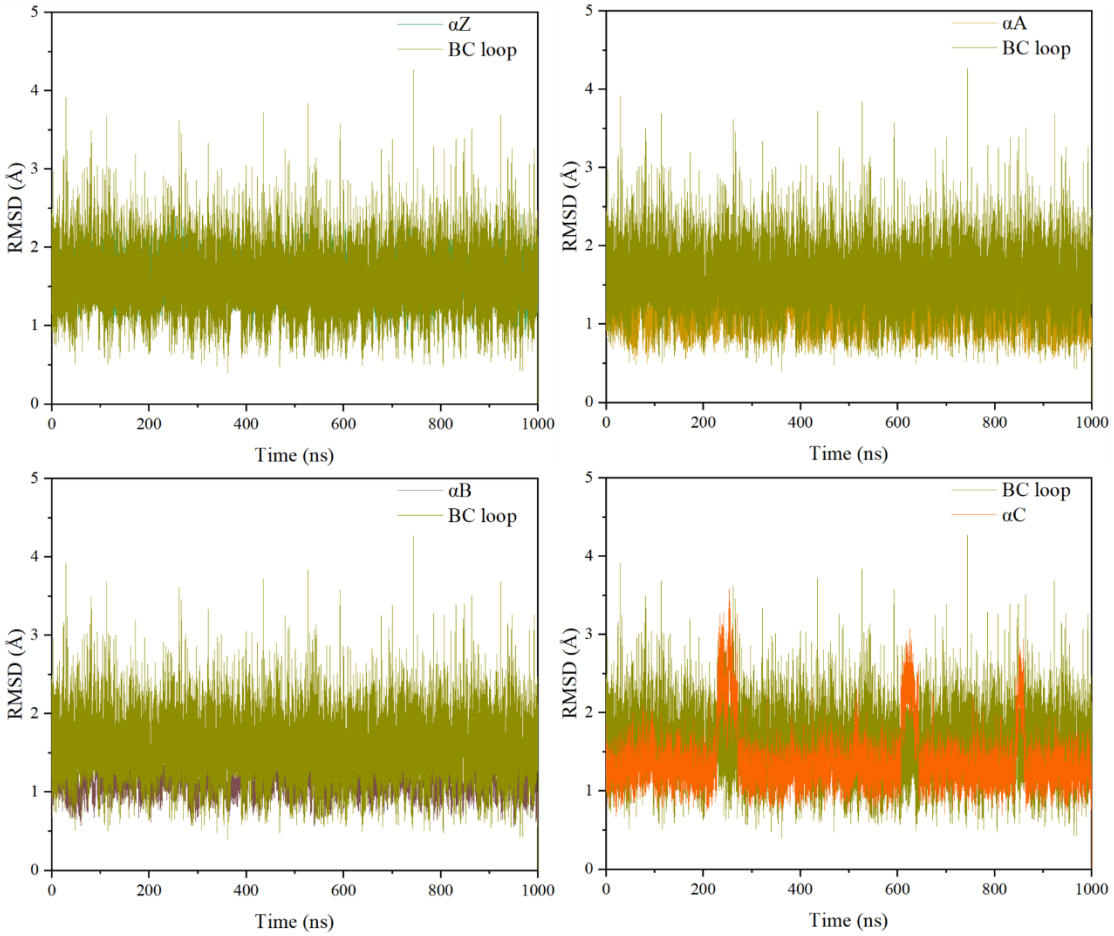

Figure S18. Root mean square deviation (RMSD) value of BC-loop compared with helices of BRD4-BD1.

Root mean square deviation (RMSD) value of non-hydrogen atoms of BC-loop calculated among the 1000 ns molecular dynamics simulation as reference with the 1000th conformation and compared with helix domains.

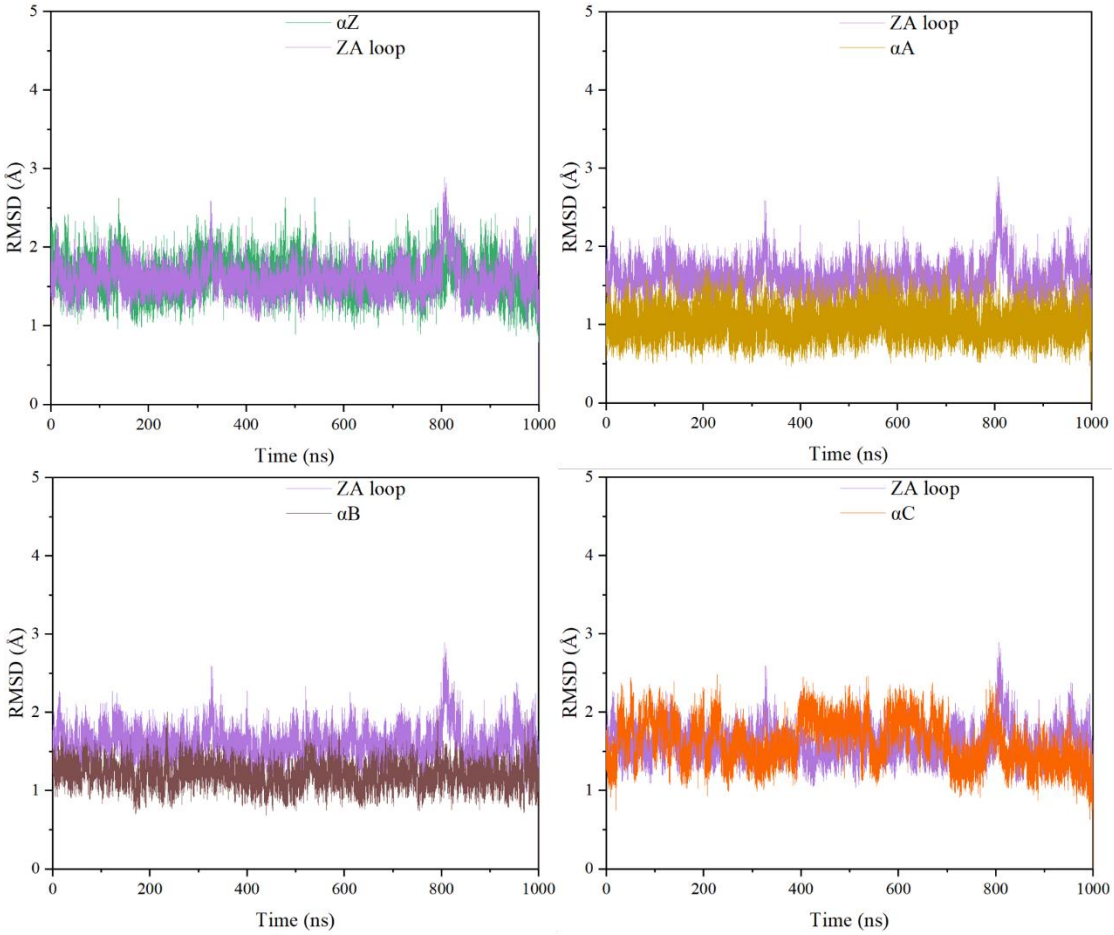

Figure S19. Root mean square deviation (RMSD) value of ZA-loop compared with helices of BRD4-BD2.

Root mean square deviation (RMSD) value of non-hydrogen atoms of ZA-loop calculated among the 1000 ns molecular dynamics simulation as reference with the 1000th conformation and compared with helix domains.

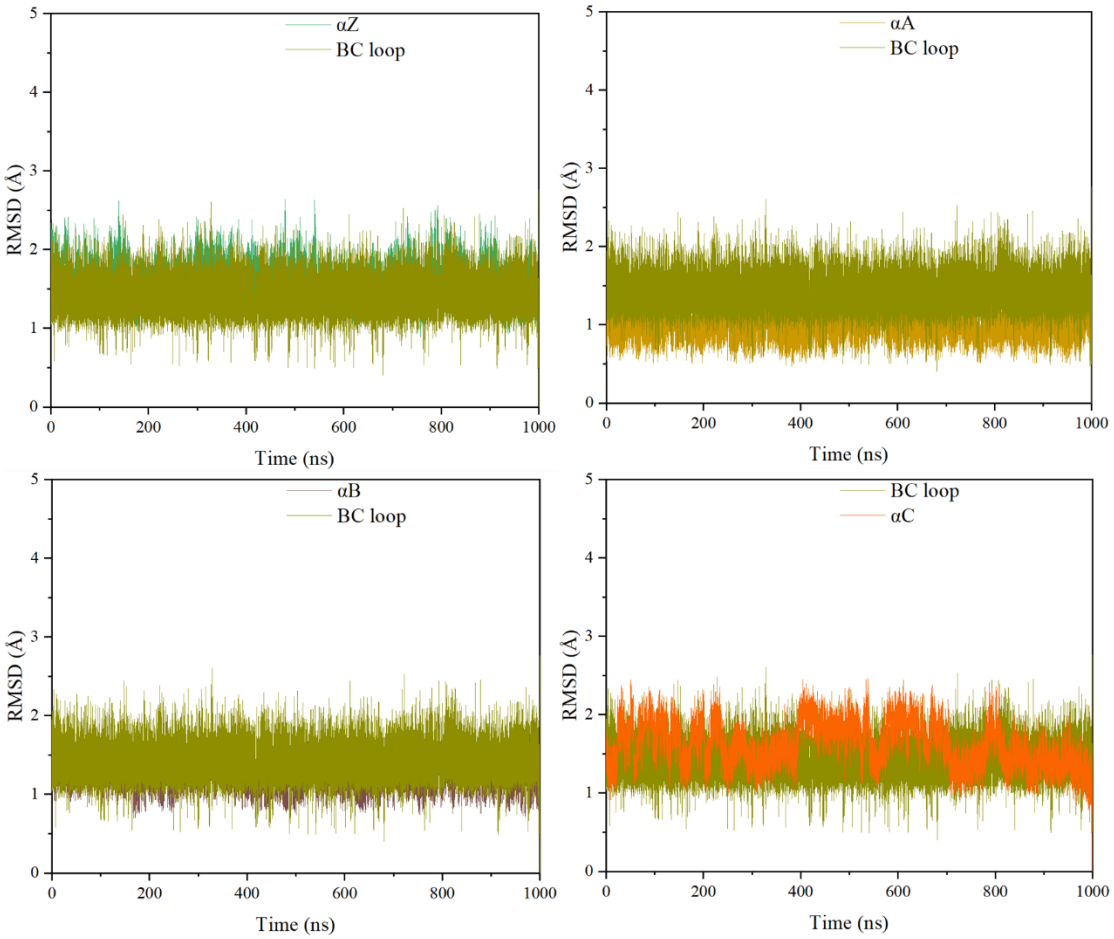

Figure S20. Root mean square deviation (RMSD) value of BC-loop compared with helices of BRD4-BD2.

Root mean square deviation (RMSD) value of non-hydrogen atoms of BC-loop calculated among the 1000 ns molecular dynamics simulation as reference with the 1000th conformation and compared with helix domains.

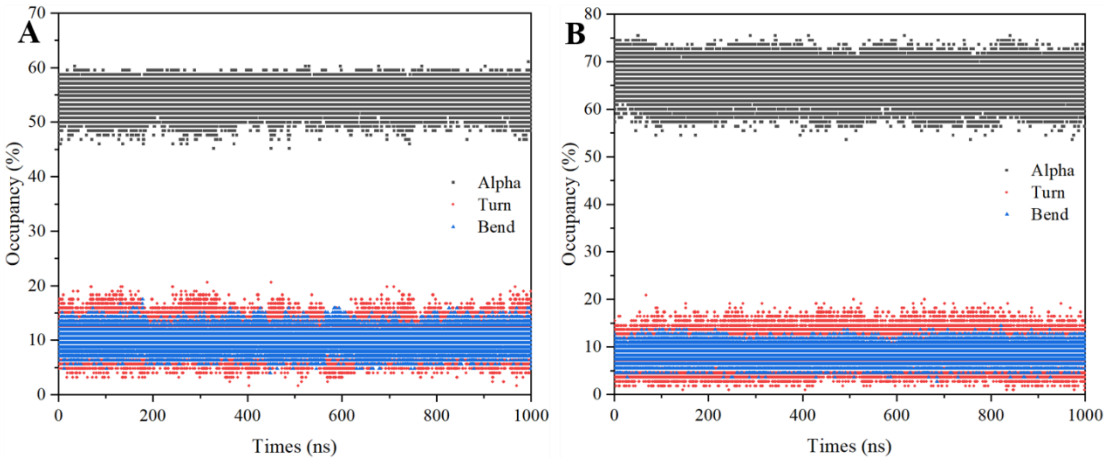

Figure S21. Secondary structure analyzed in the simulation of NHWD-870/BRD4-BD1 (A) and BD2 (B) systems.

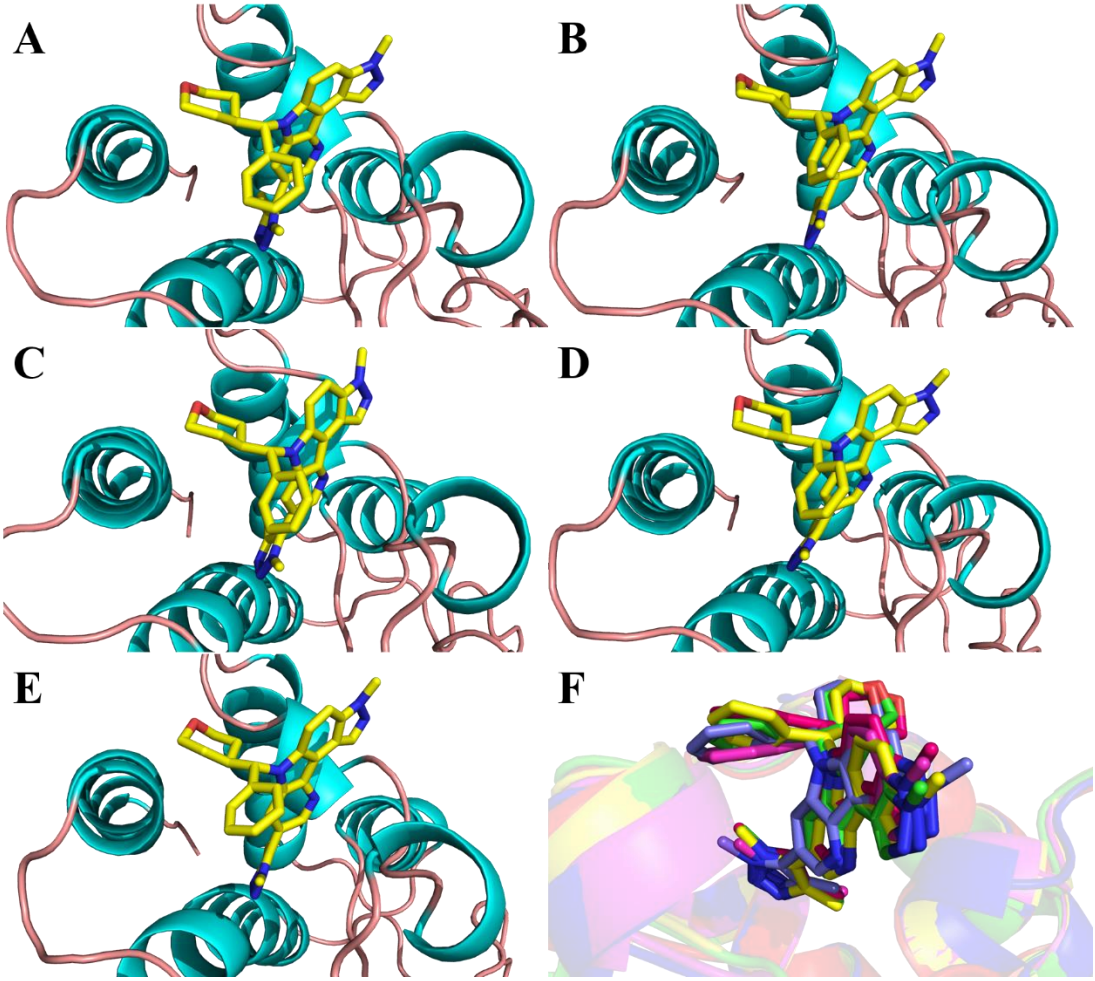

Figure S22. Snapshots of the NHWD-870/BRD4-BD1 along the dynamic simulation time for 200 ns (A), 400 ns (B), 600 ns (C), 800 ns (D), 1000 ns (E) and align them(F). For clarity, the water molecules have been removed. The NHWD-870 is plotted using stick style, while cartoon style for BRD4-BD1.

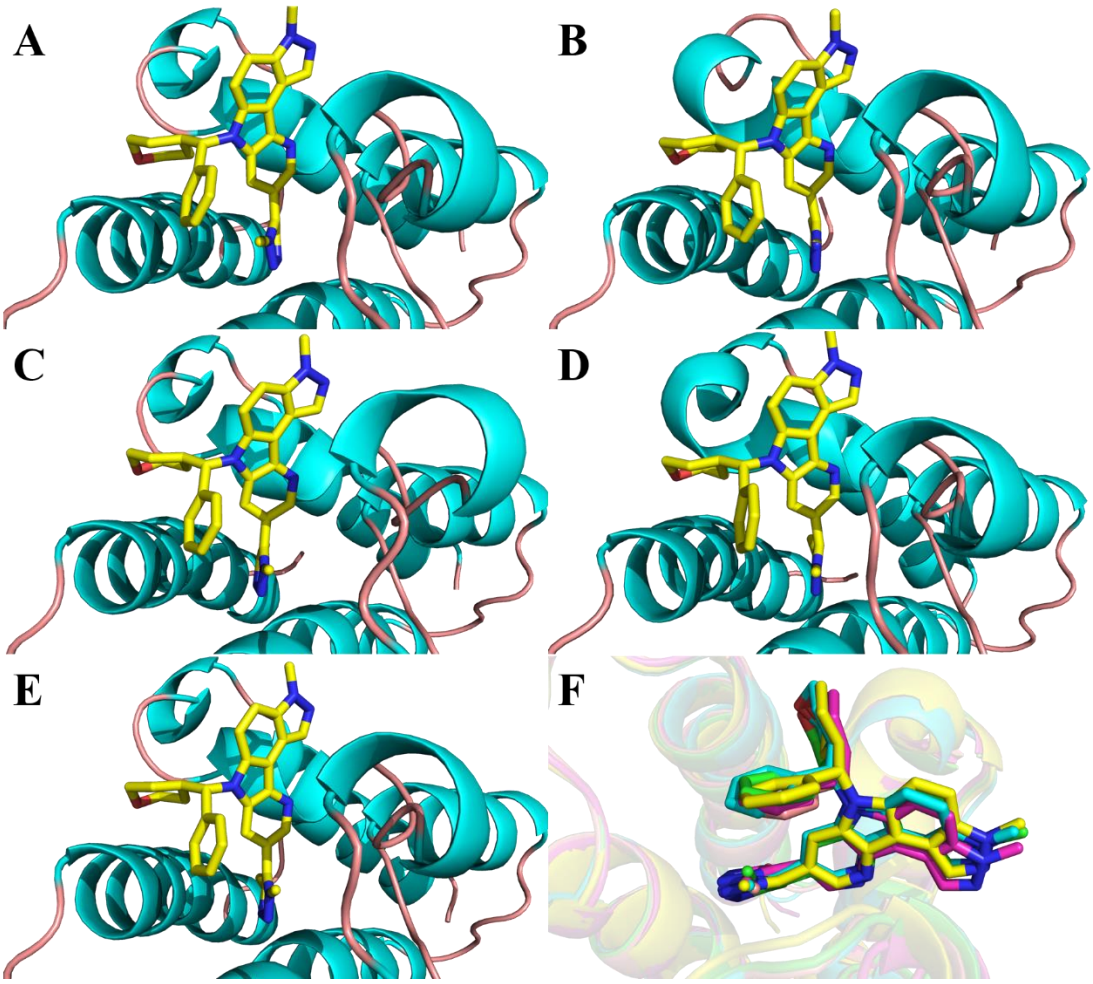

Figure S23. Snapshots of the NHWD-870/BRD4-BD2 along the dynamic simulation time for 200 ns (A), 400 ns (B), 600 ns (C), 800 ns (D), 1000 ns (E) and align them(F). For clarity, the water molecules have been removed. The NHWD-870 is plotted using stick style, while cartoon style for BRD4-BD2.

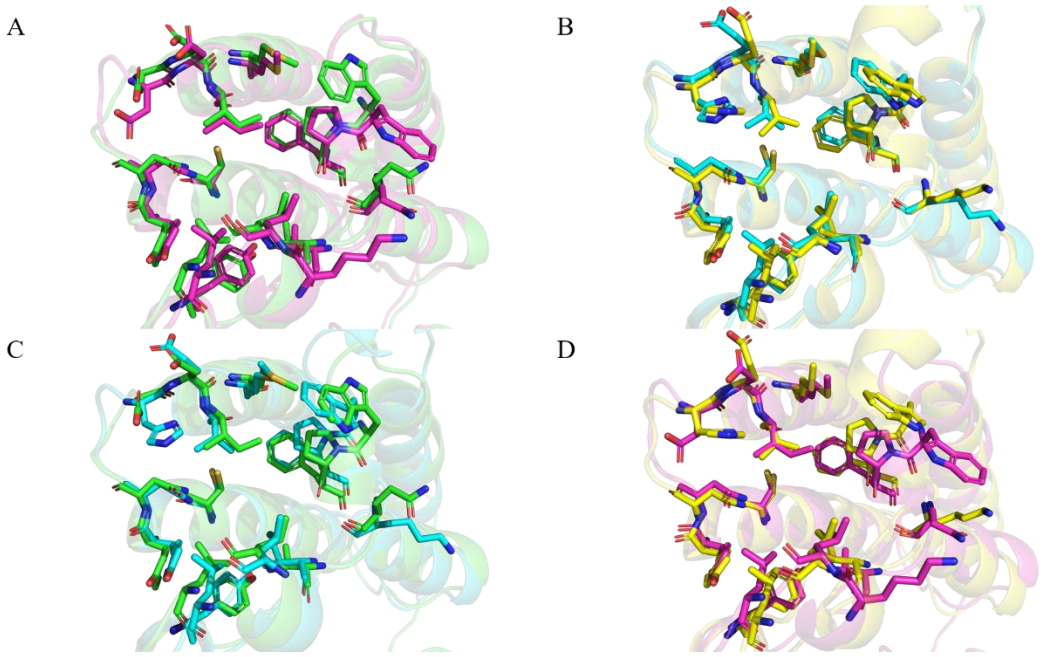

Figure S24. The structures for 1000th snapshot and initial frame of the NHWD-870/BRD4 complex systems.

The residues around 4 Å from the NHWD-870 was shown with stick. The BRD4-BD1 or BRD4-BD2 was shown with cartoon. The initial frame of NHWD-870/BRD4-BD1 shown with magenta, initial frame of NHWD-870/BRD4-BD2 with yellow, 1000th snapshot of NHWD-870/BRD4-BD1 with green, and 1000th snapshot of NHWD-870/BRD4-BD1 with cyan.

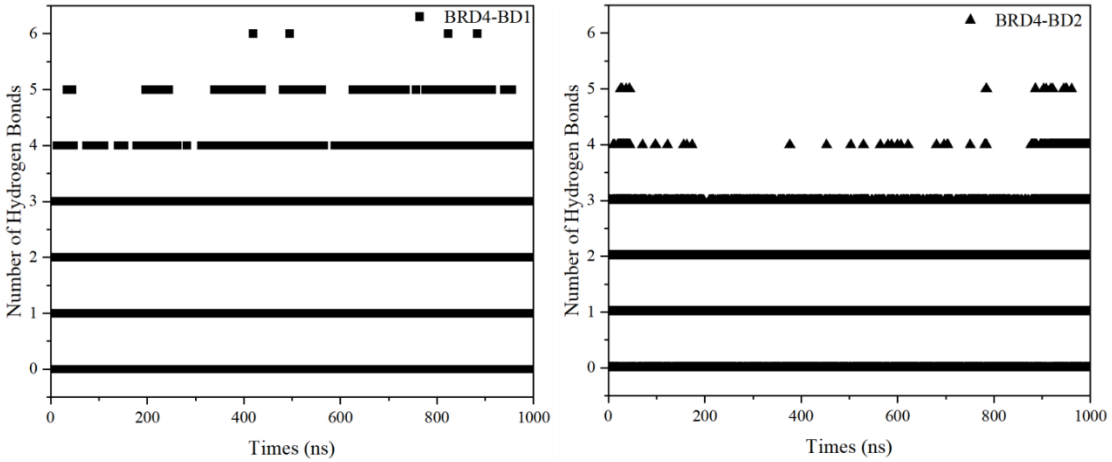

Figure S25. Statistical hydrogen bond number profile along the 1000-ns MD simulation for NHWD-870/BRD-BD1 and BD2.

Hydrogen bond is defined as the distance between the acceptor and donor atoms < 3.5 Å, with an internal angle between the H-acceptor and H-donor > 120º.

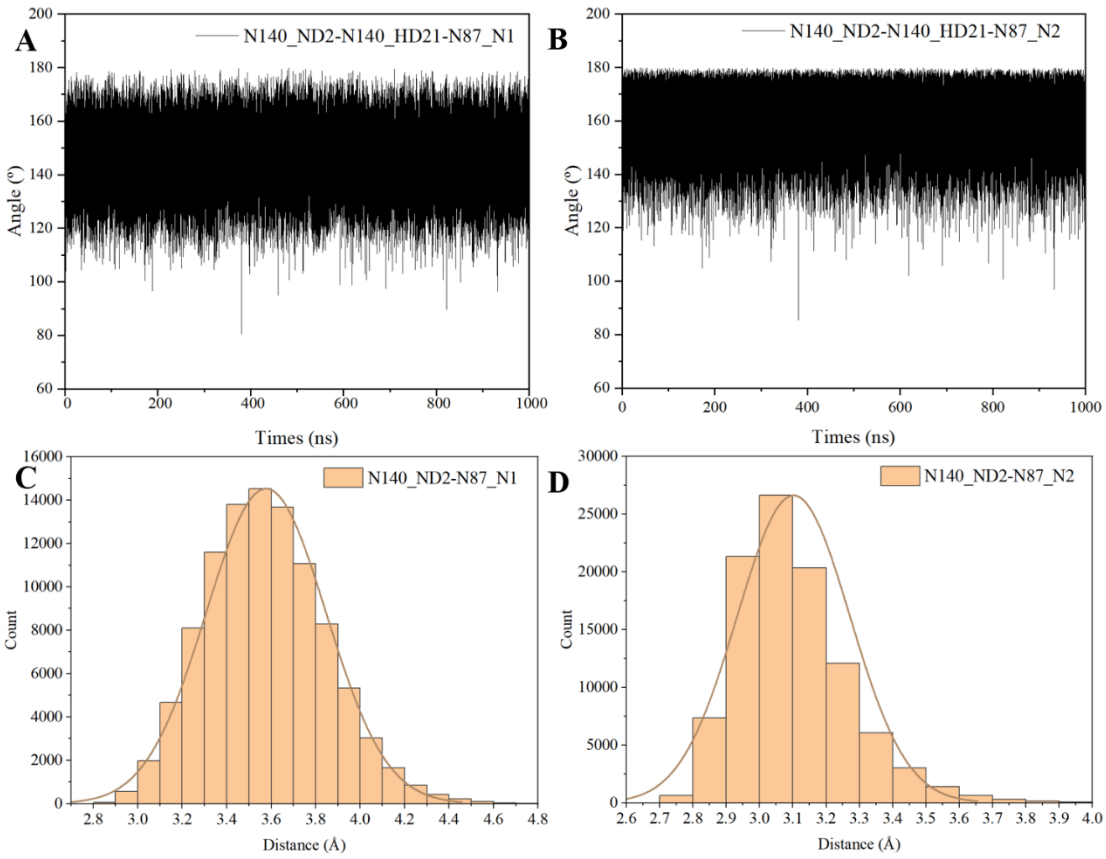

Figure S26. The angle and distance of hydrogen bonds between NHWD-870 (N87) and BRD4-BD1.

(A) for the angle of N140_ND2-N140_HD21-N87_N1; (B) for angle of N140_ND2-N140_HD21-N87_N2; (C) for the distance distribution of N140_ND2 -N87_N1; (D) for distance distribution of N140_ND2 -N87_N2.

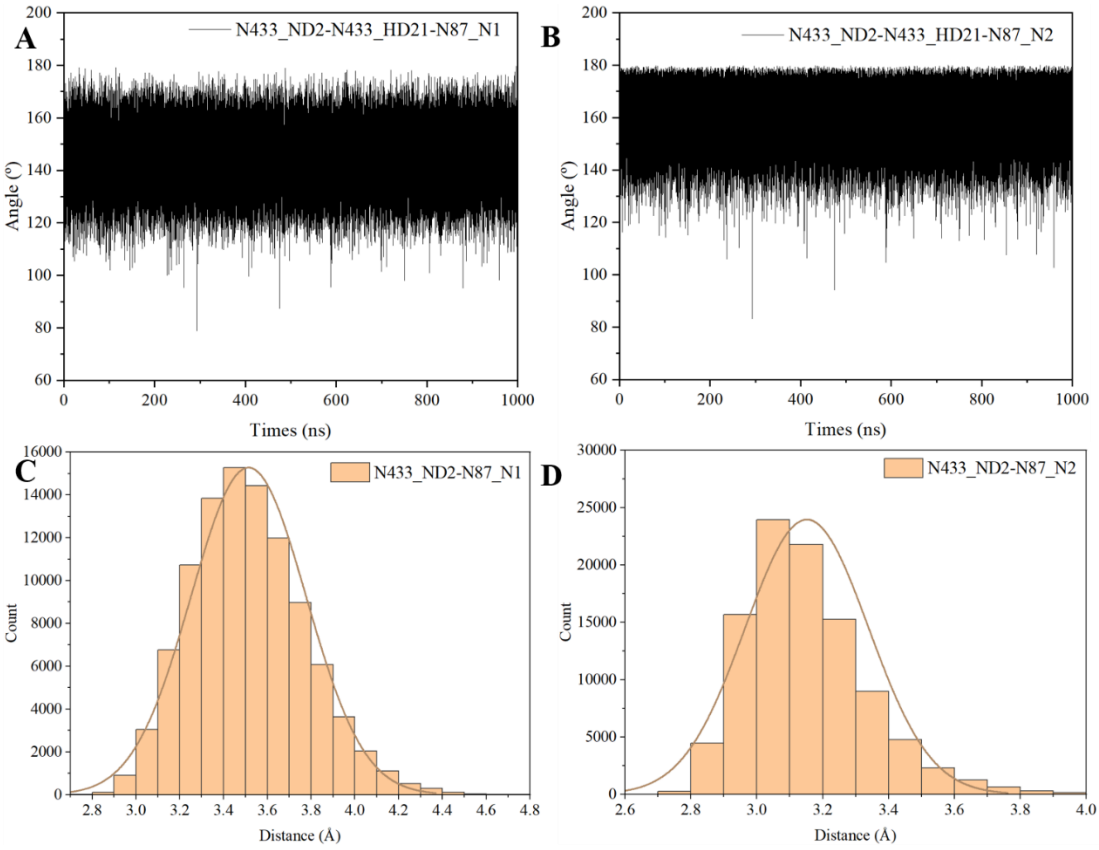

Figure S27. The angle and distance of hydrogen bonds between NHWD-870 (N87) and BRD4-BD2.

(A) for the angle of N433_ND2-N433_HD21-N87_N1; (B) for angle of N433_ND2-N433_HD21-N87_N2; (C) for the distance distribution of N433_ND2 -N87_N1; (D) for distance distribution of N433_ND2 -N87_N2.

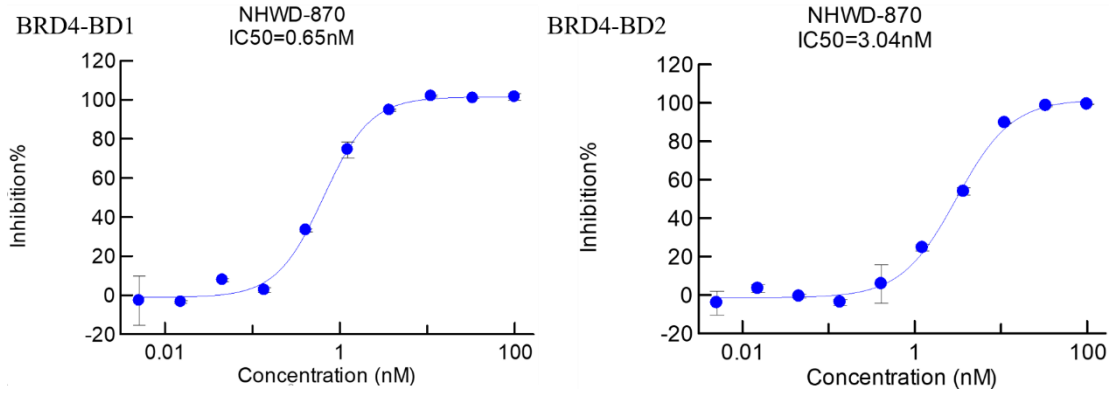

Figure S28. The biochemical activity of NHWD-870 against BRD4-BD1 and BRD4-BD2.

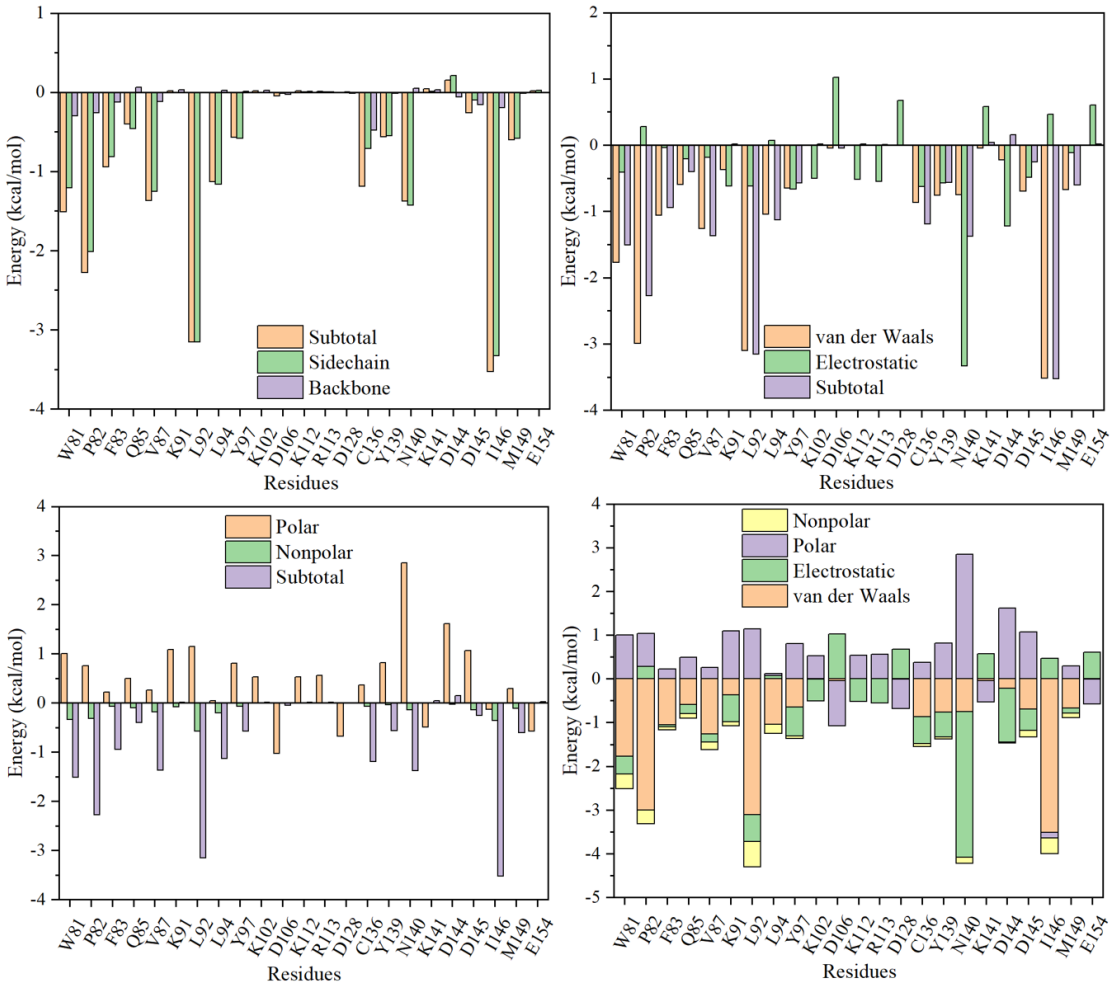

Figure S29. The decomposition energy for NHWD-870 with BRD4-BD1.

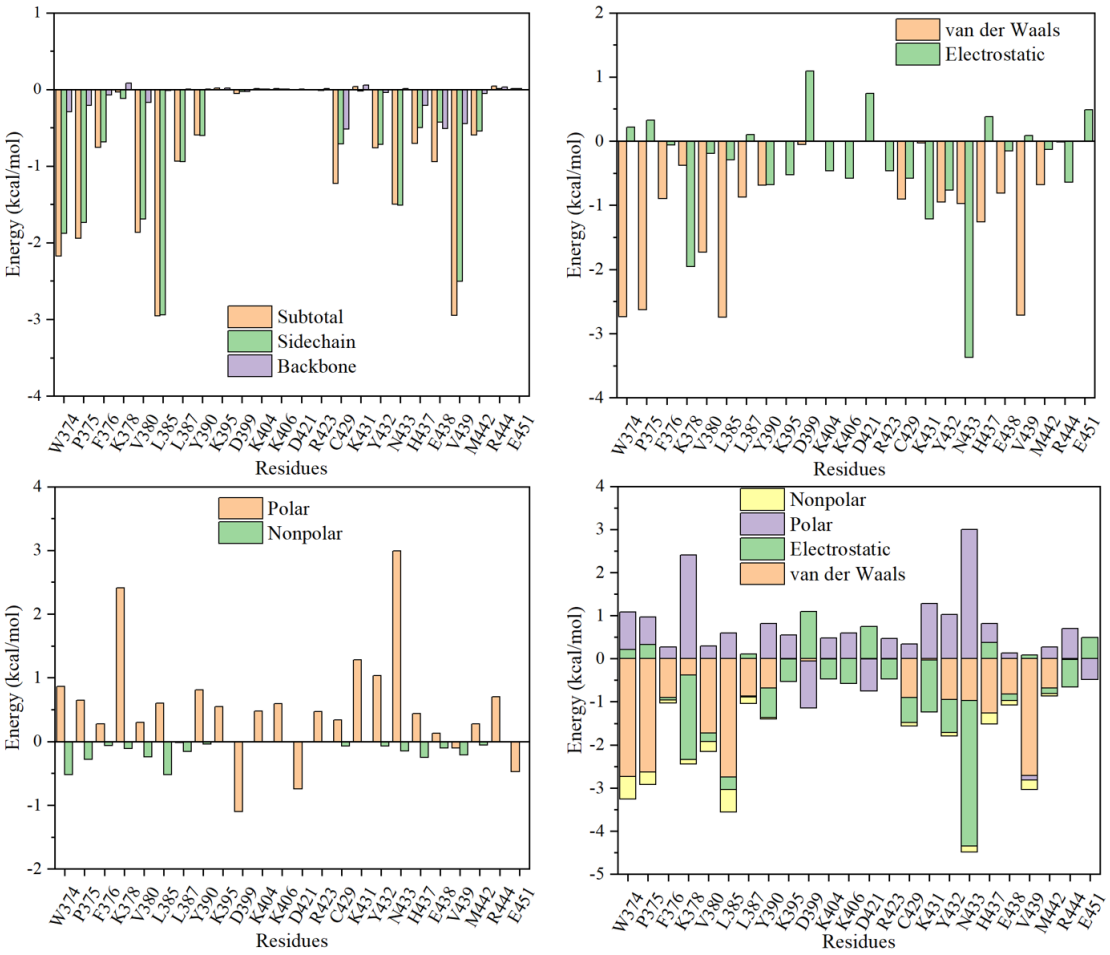

Figure S30. The decomposition energy for NHWD-870 with BRD4-BD1.

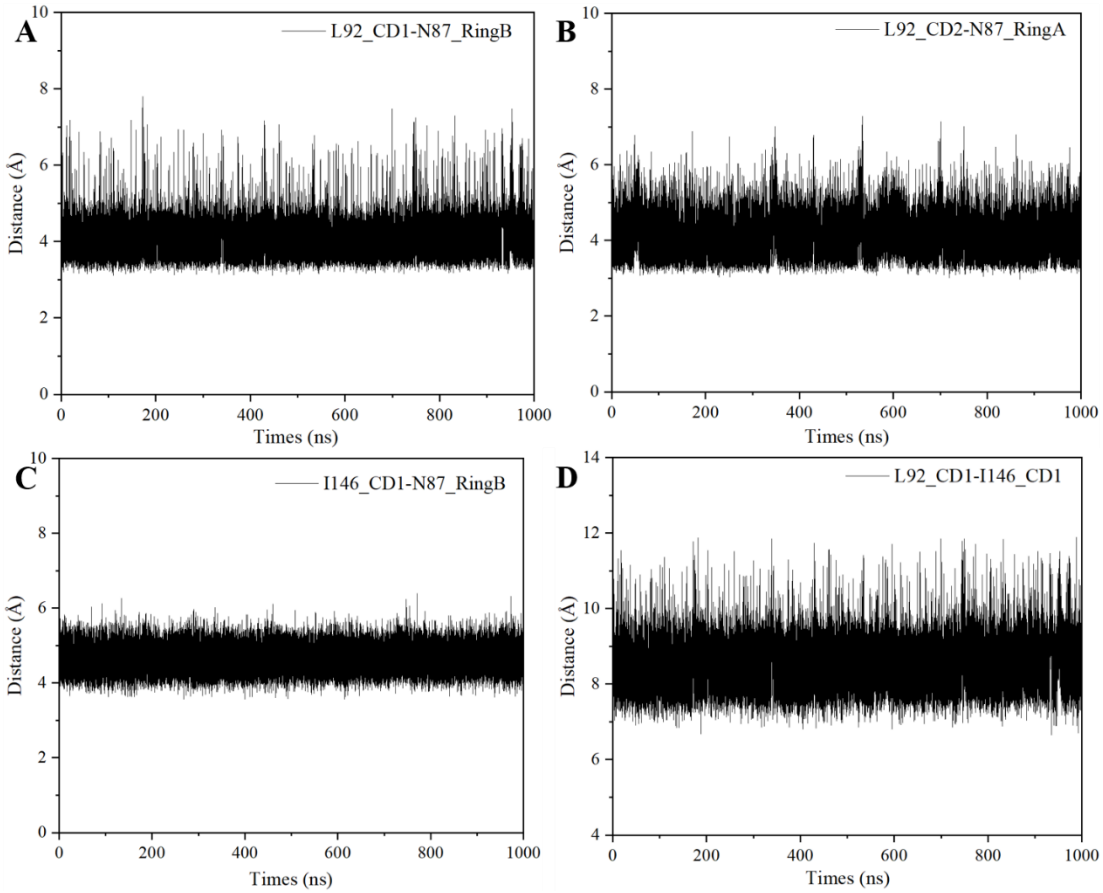

Figure S31. The distance between L92 or I146 with NHWD-870 in NHWD-870/BRD4-BD1.

(A) for distance between L92 with ring B of NHWD-870; (B) for distance between L92 with ring A of NHWD-870; (C) for distance between I146 with ring B of NHWD-870; (D) for distance between L92 with I146.

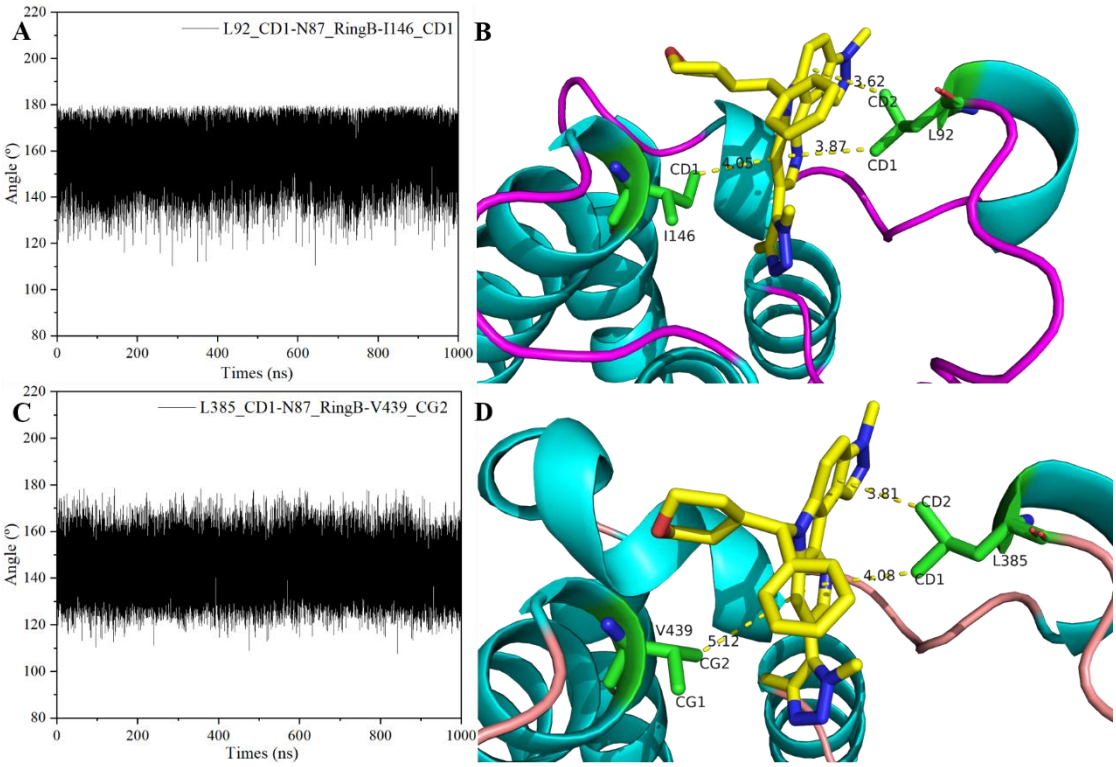

Figure S32. The angle among L92-Ring B-I146 and L385-Ring B-V439.

(A) for angle among L92, ring B of NHWD-870, and I146; (B) for schema of L92-Ring B-I146; (C) for angle among L385, ring B, and V439; (D) for schema of L385-Ring B-V439.

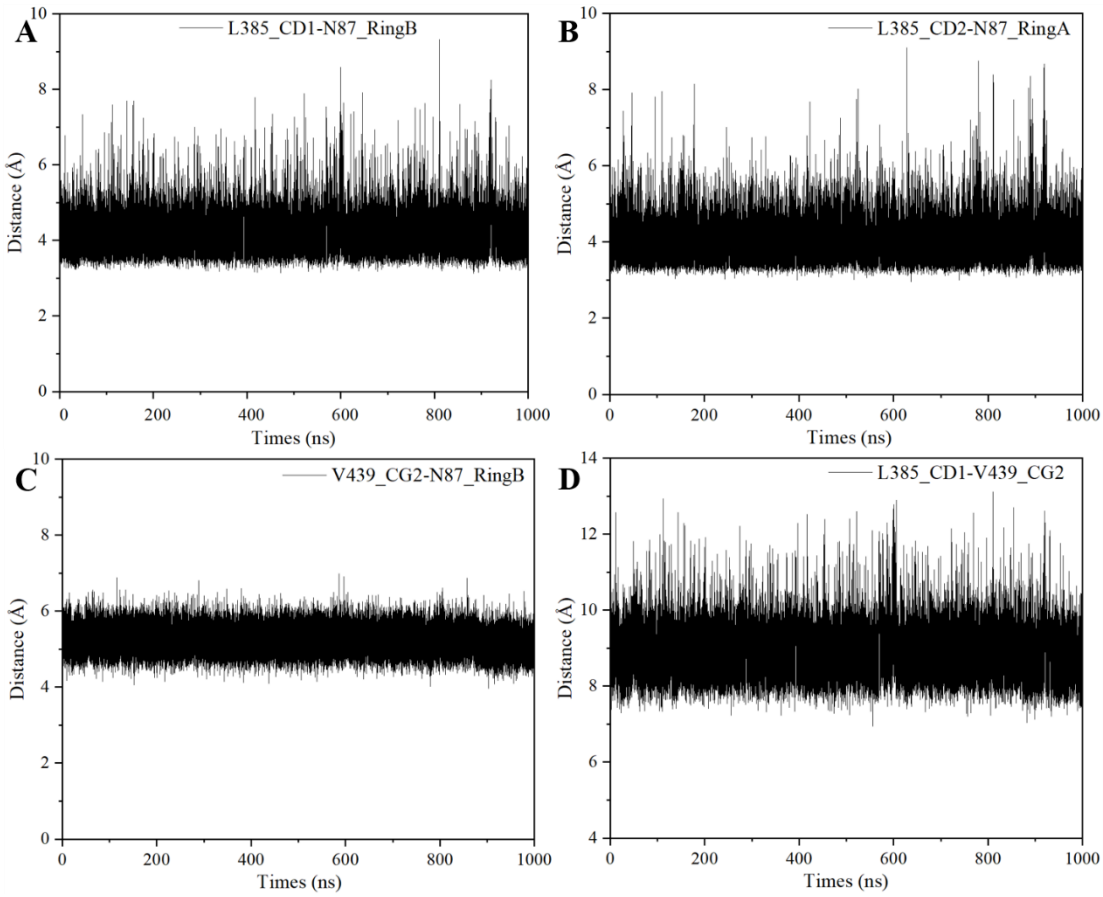

Figure S33. The distance between L385 or V439 with NHWD-870 in NHWD-870/BRD4-BD2.

(A) for distance between L385 with ring B of NHWD-870; (B) for distance between L385 with ring A of NHWD-870; (C) for distance between V439 with ring B of NHWD-870; (D) for distance between L385 with V439.

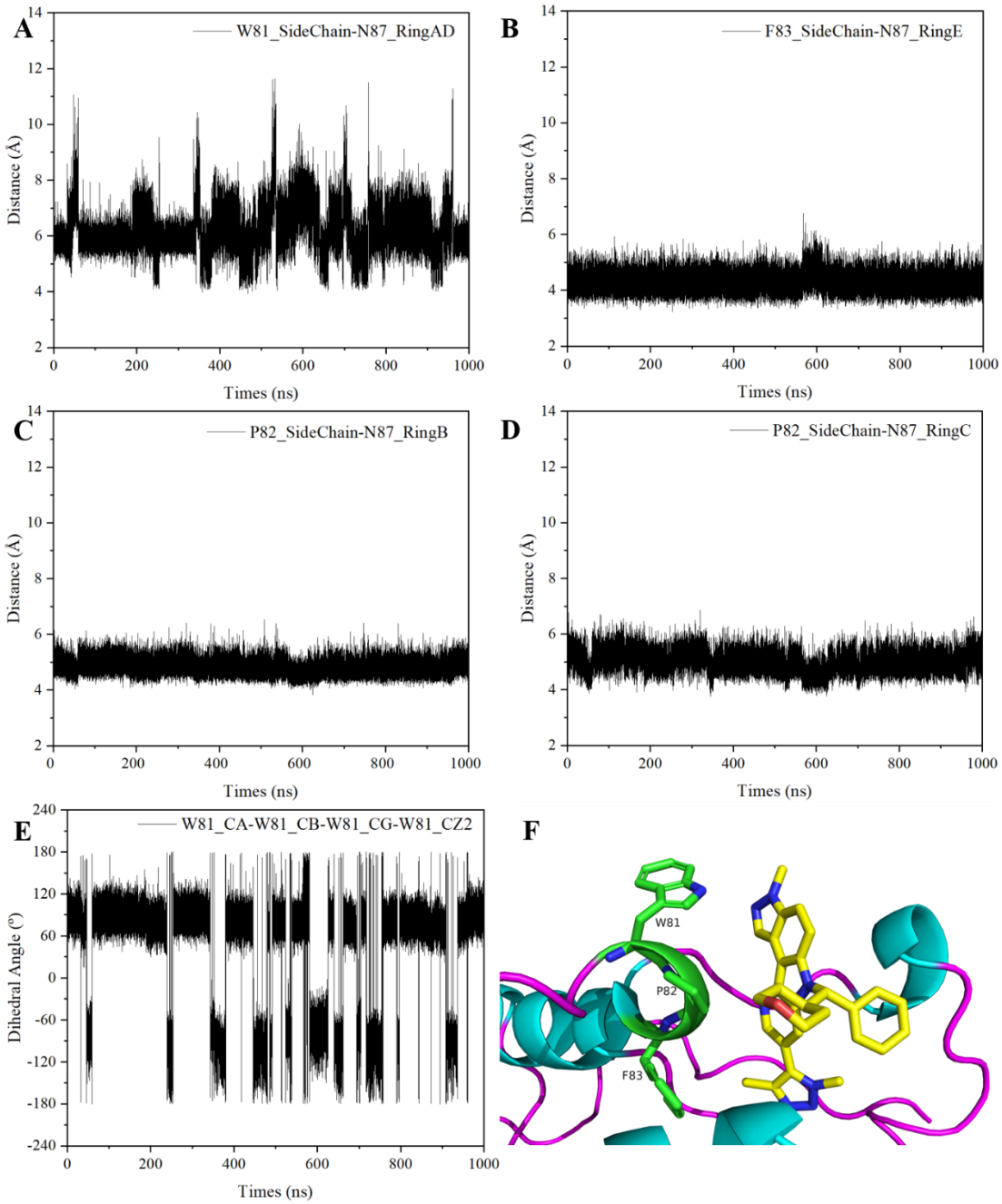

Figure S34. The analysis for W81, P82, F83 with the NHWD-870.

(A) for distance between W81 with ring A and D; (B) for distance F83 with ring E; (C) for distance between P82 with ring B; (D) for distance between P82 with ring C; (E) for dihedral angle among W81_CA, W81_CB, W81_CG, and W81_CZ2; (F) for the schema for W81, P82, and F83.

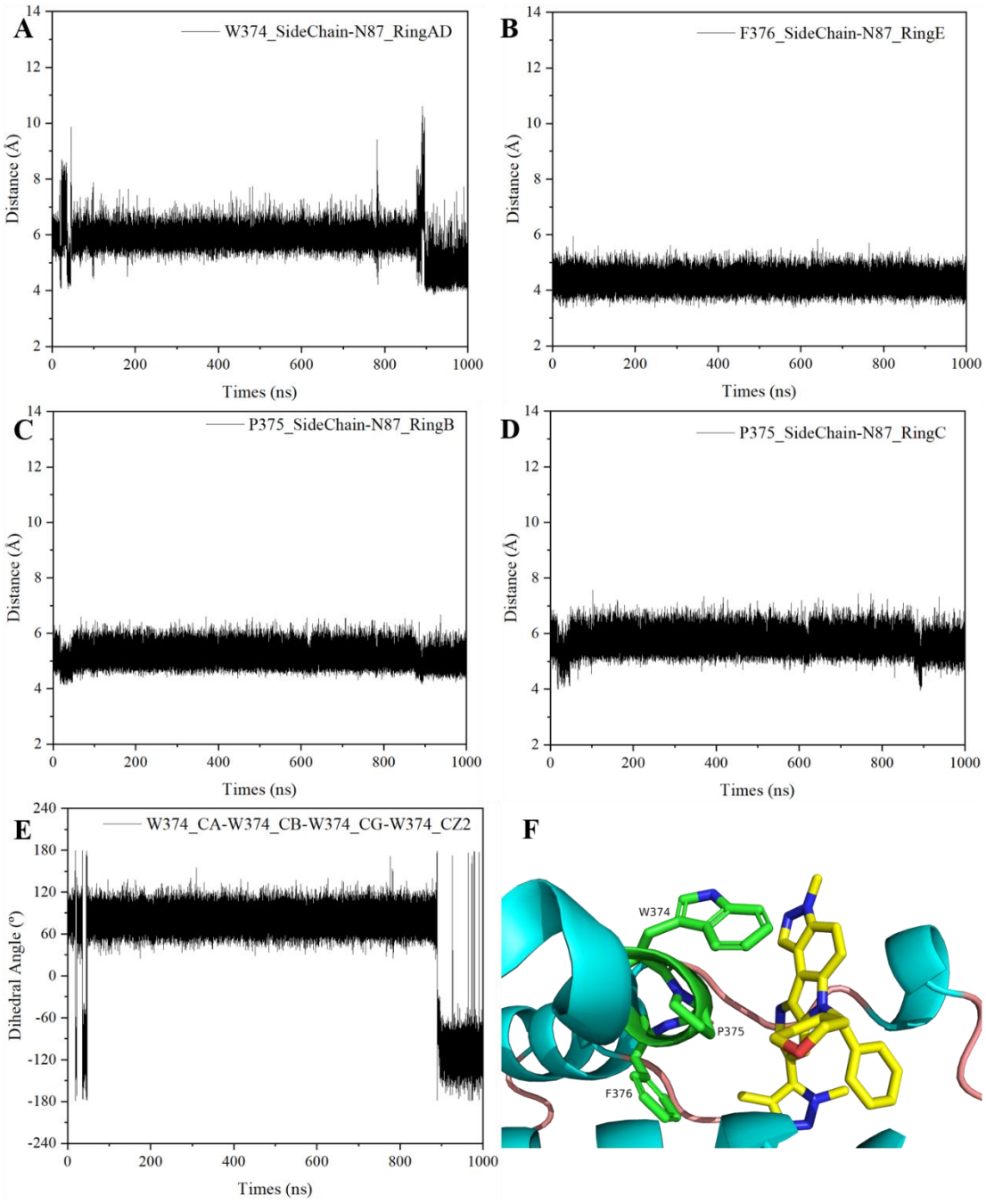

Figure S35. The analysis for W374, P375, F376 with the NHWD-870.

(A) for distance between W374 with ring A and D; (B) for distance F376 with ring E; (C) for distance between P375 with ring B; (D) for distance between P375 with ring C; (E) for dihedral angle among W374_CA, W374_CB, W374_CG, and W374_CZ2; (F) for the schema for W374, P375, and F376.

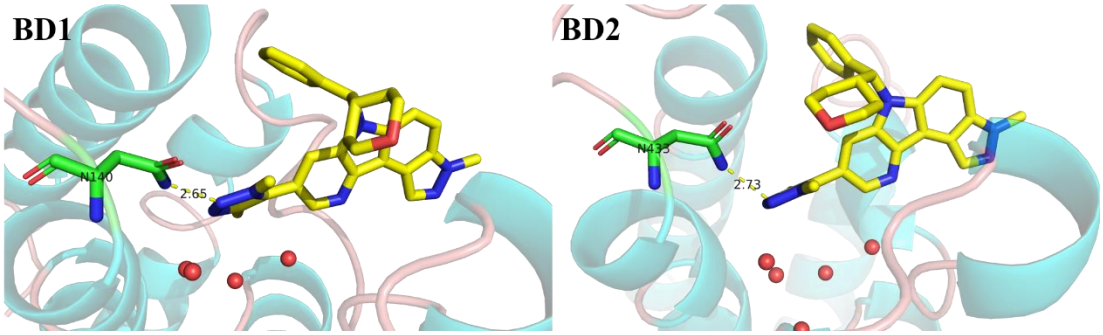

Figure S36. Docking results for NHWD-870-R with BRD4-BD1 and BD2.

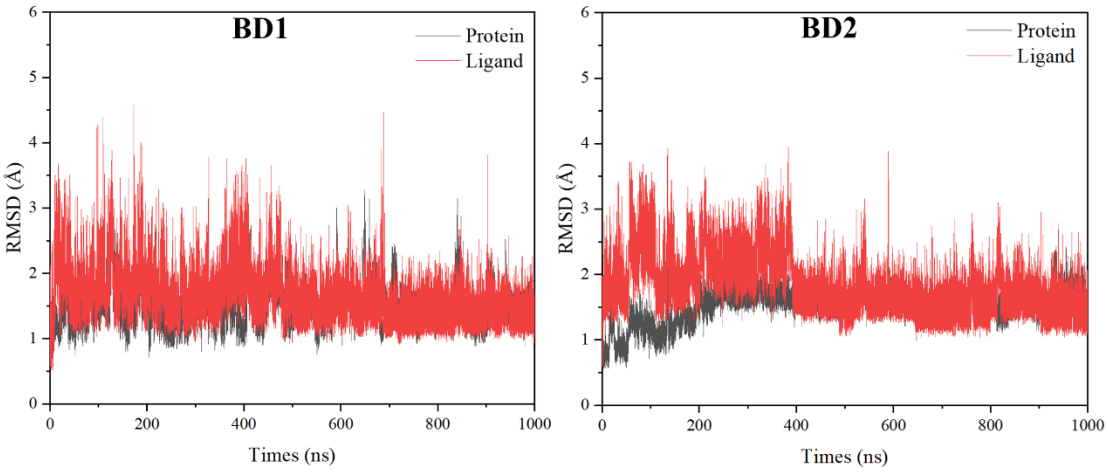

Figure S37. The root mean square deviation (RMSD) value of heavy atoms of backbone of protein and heavy atoms of inhibitor along 1000 ns MD simulations for NHWD-870-R with BRD4-BD1 and BD2.

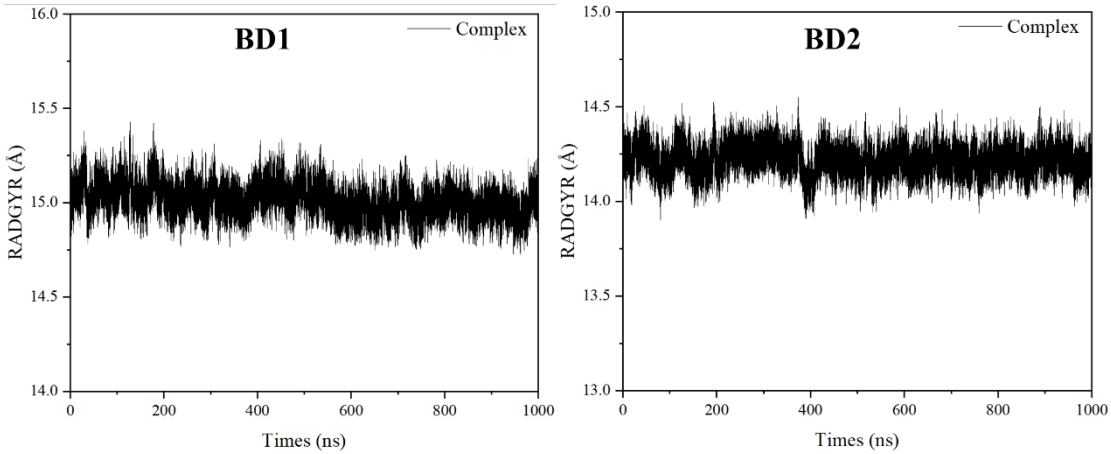

Figure S38. The gyration radius (RADGYR) of complex systems for NHWD-870-R with BRD4-BD1 and BD2.

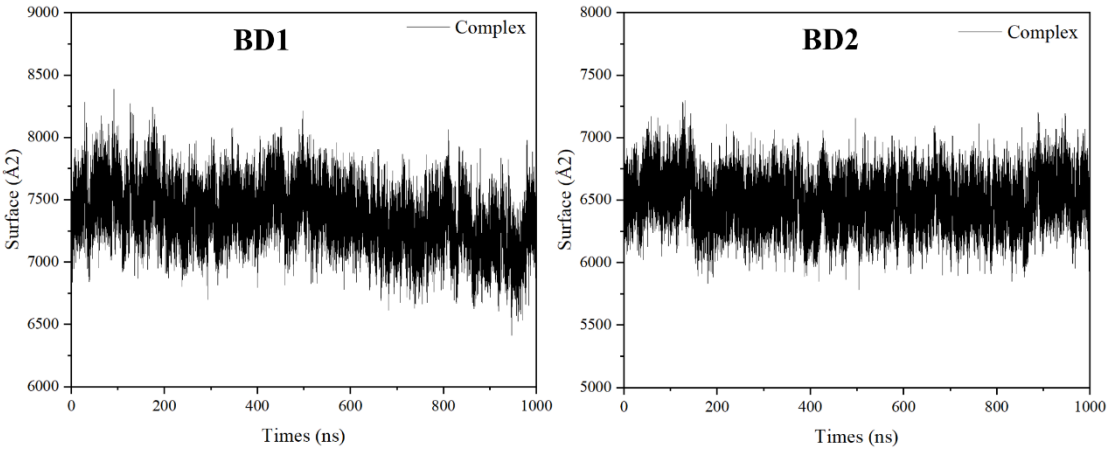

Figure S39. The surface of NHWD-870-R with BRD4-BD1and BD2.

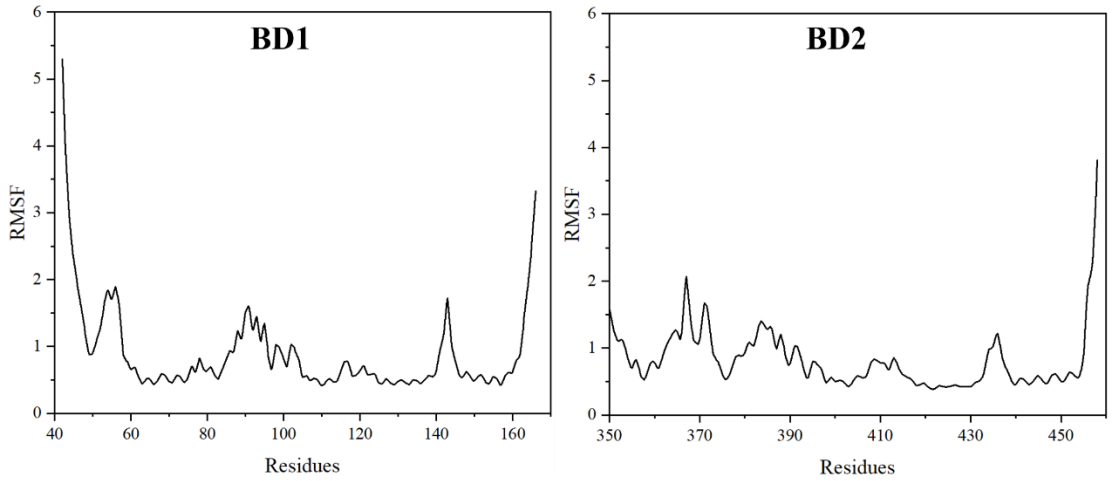

Figure S40. The RMSF value for protein of BD1 or BD2 of BRD4 with NHWD-870-R in the MD simulation.

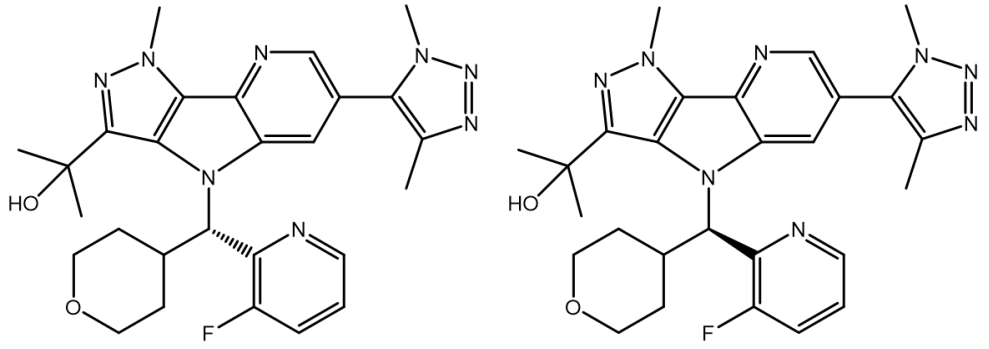

Compound 1-S

IC_{50} 0.97 nM

Compound 1-R

IC_{50} 3.00 nM

Figure S41. The structure of Compound 1 with R and S stereochemical structure.

The IC_{50} extracted from Fang, H.; Chen, M.; Yang, G.; Du, Y.; Wang, Y.; Wu, T.; Li, Q.; Zhang, L.; Hu, S. New fused heterocyclic derivatives are bromodomain and extra-terminal inhibitors used to treat solid tumor e.g. lung cancer, colon cancer, rectal cancer, colorectal cancer and ovarian cancer and/or blood tumor e.g. myeloma and/or leukemia. WO2020001152-A1.

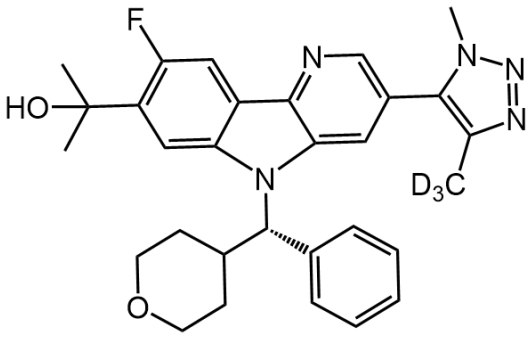

A1

IC_{50}: 0.9 nM

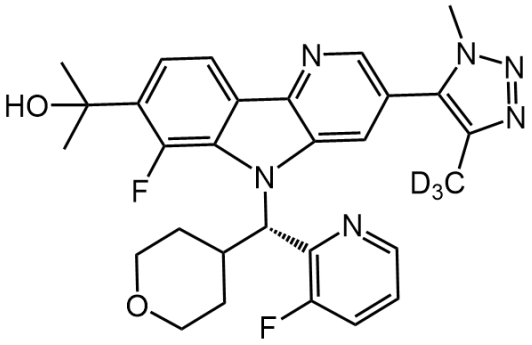

A2

IC_{50}: 0.9 nM

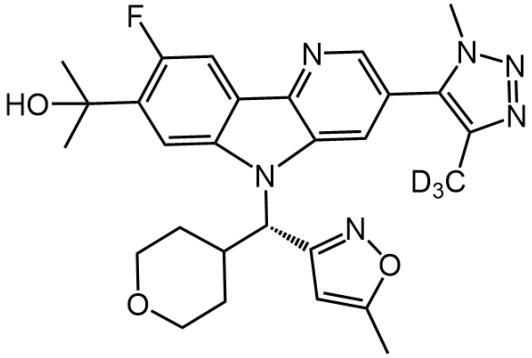

A3

IC_{50}: 1.4 nM

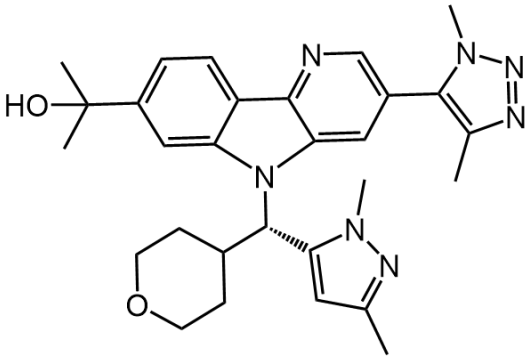

A4

IC_{50}: 2.3 nM

Figure S42. The structure of Compound A1-A4 and their IC_{50} values.

The IC_{50} extracted from Hill, M. D.; Fang, H.; Tokarski, J.; Fanslau, C.; Haarhoff, Z.; Huang, C.; Kramer, M.; Menard, K.; Monereau, L.; Morrison, J.; Ranasinghe, A.; Shields, E. E.; Tye, C. K.; Westhouse, R.; Everlof, G.; Sheriff, S.; Yan, C.; Marsilio, F.; Zhang, L.; Zvyaga, T.; Lee, F.; Gavai, A. V.; Degnan, A. P., Development of BET inhibitors as potential treatments for cancer: A search for structural diversity. Bioorganic & Medicinal Chemistry Letters 2021, 44, 128108.

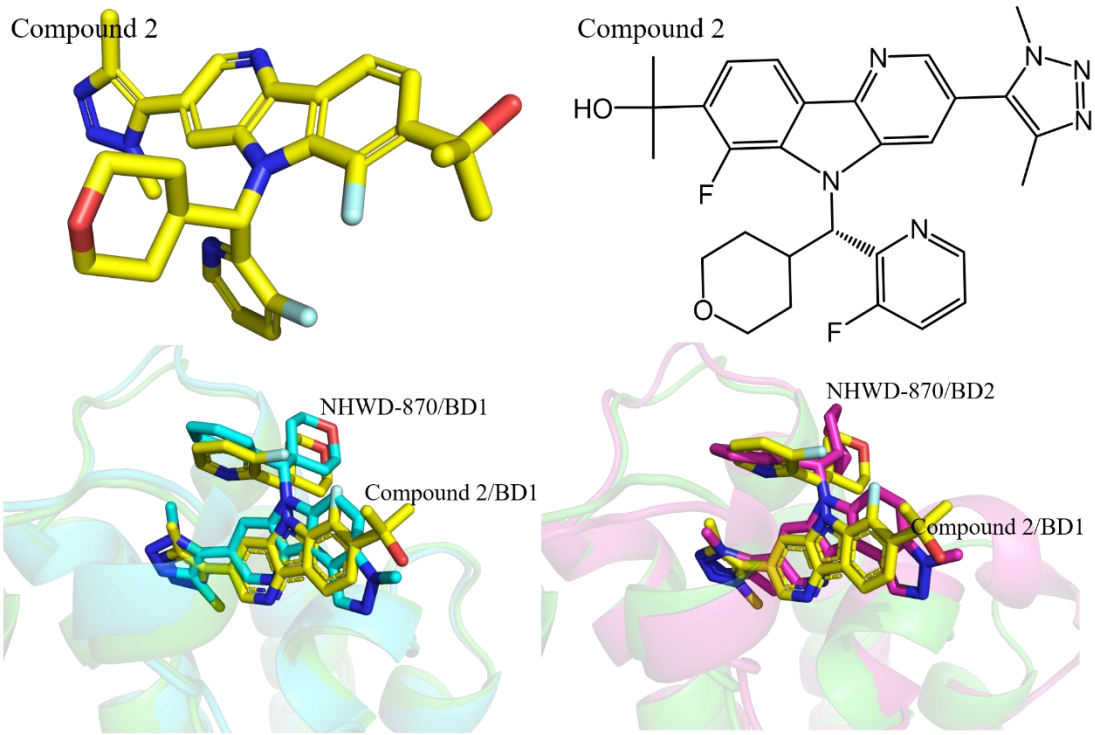

Figure S43. The structure of Compound 2 and binding model with BRD4-BD1.

The crystal complex structure for Compound 2 with BRD4-BD1 was extracted from the Protein Database Band (PDB IC: 7MCF). The complex structures for NHWD-870 with BRD4-BD1/BD2 were obtained from our MD simulations and can be obtained from the supporting information.

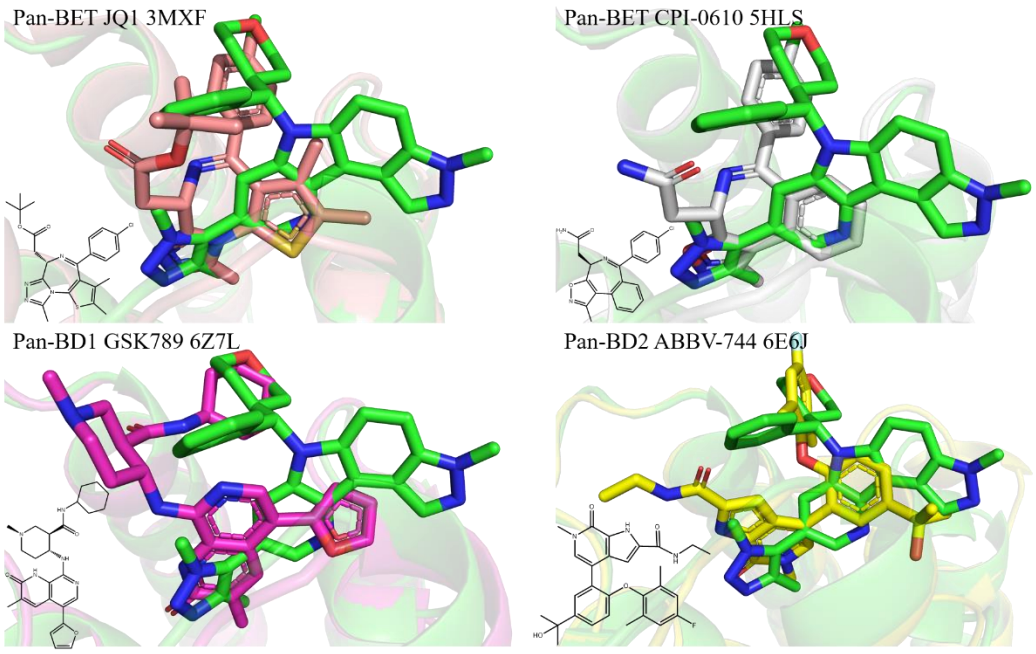

Figure S44. The superposition between NHWD-870/BRD4-BD1 (green) with JQ1/BRD4-BD1 (wheat, 3MXF), CPI-0610/BRD4-BD1 (gray, 5HLS), GSK789/BRD4-BD1 (magenta, 6Z7L), and ABBV-744/BRD4-BD2 (yellow, 6E6J).

JQ1/BRD4-BD1: Nature 2010, 468 (7327), 1067-1073.

CPI-0610/BRD4-BD1: Journal of Medicinal Chemistry 2016, 59 (4), 1330-1339.

GSK789/BRD4-BD1: Journal of Medicinal Chemistry 2020, 63 (17), 9045-9069.

ABBV-744/BRD4-BD2: Nature 2020, 578 (7794), 306-311.

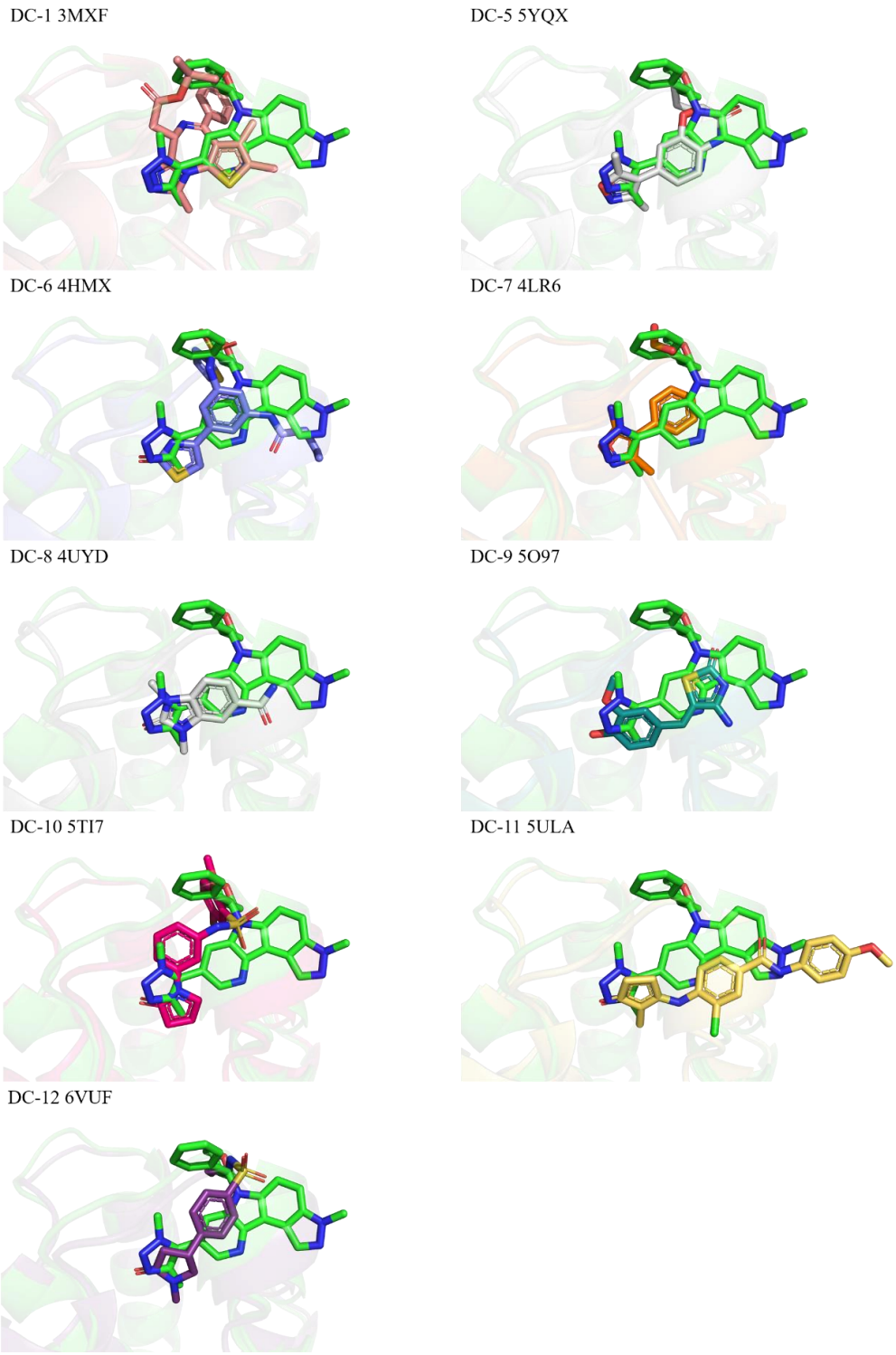

Figure S45. The designing strategies for the novel compounds.

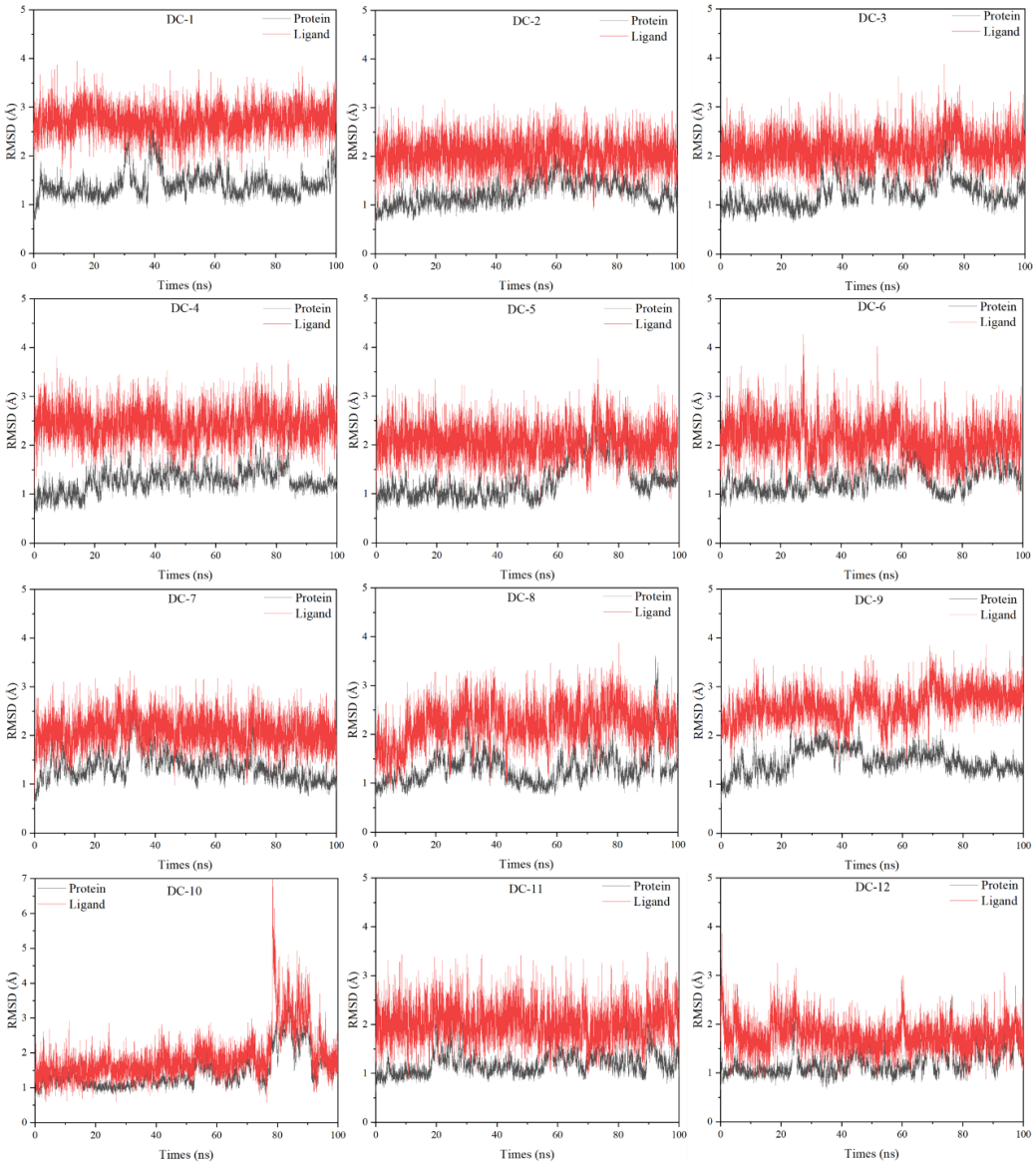

Figure S46. The root mean square deviation (RMSD) value of heavy atoms of backbone of protein and heavy atoms of inhibitor along 100 ns MD simulations for designed compounds with BRD4-BD1.

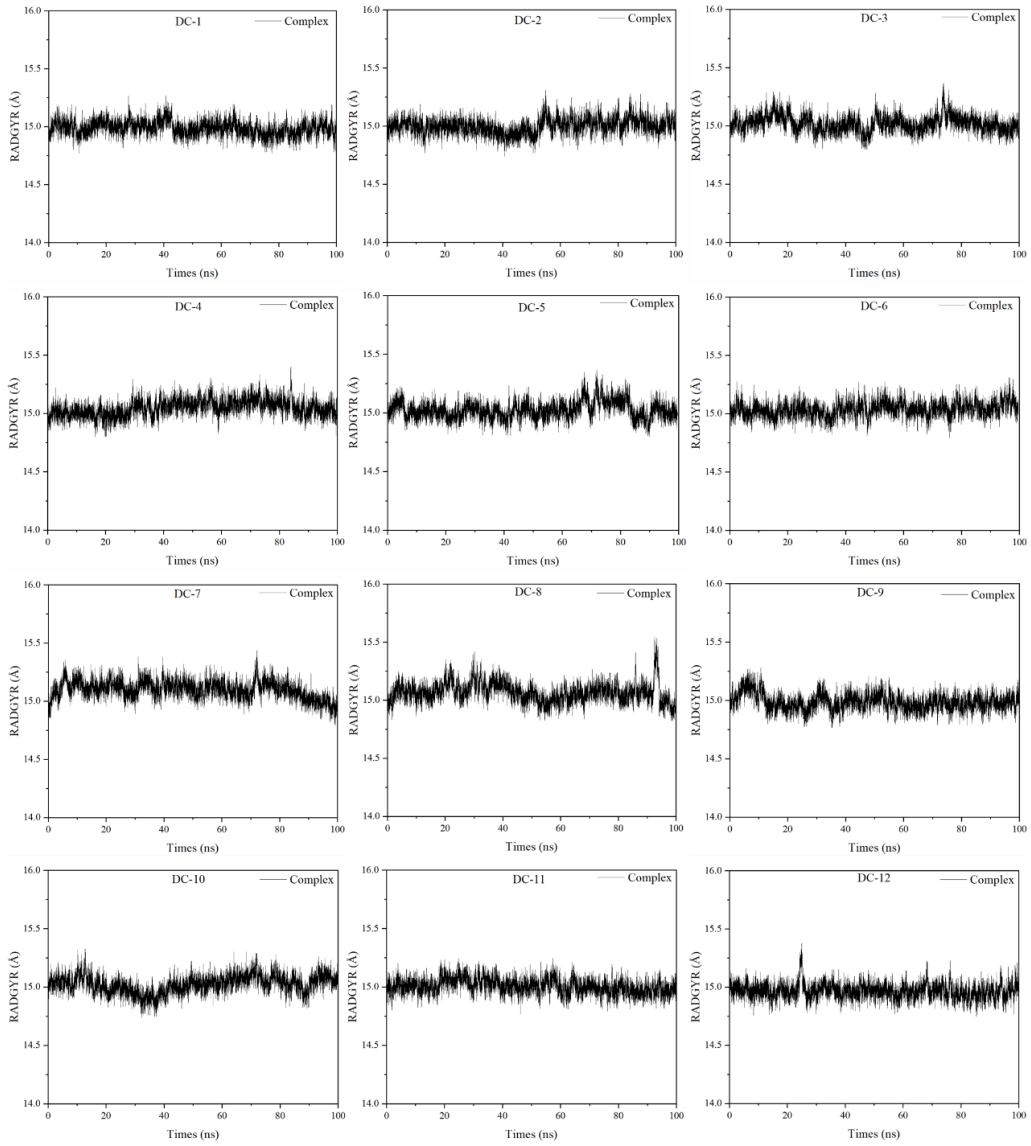

Figure S47. The gyration radius (RADGYR) of designed compounds with BRD4-BD1.

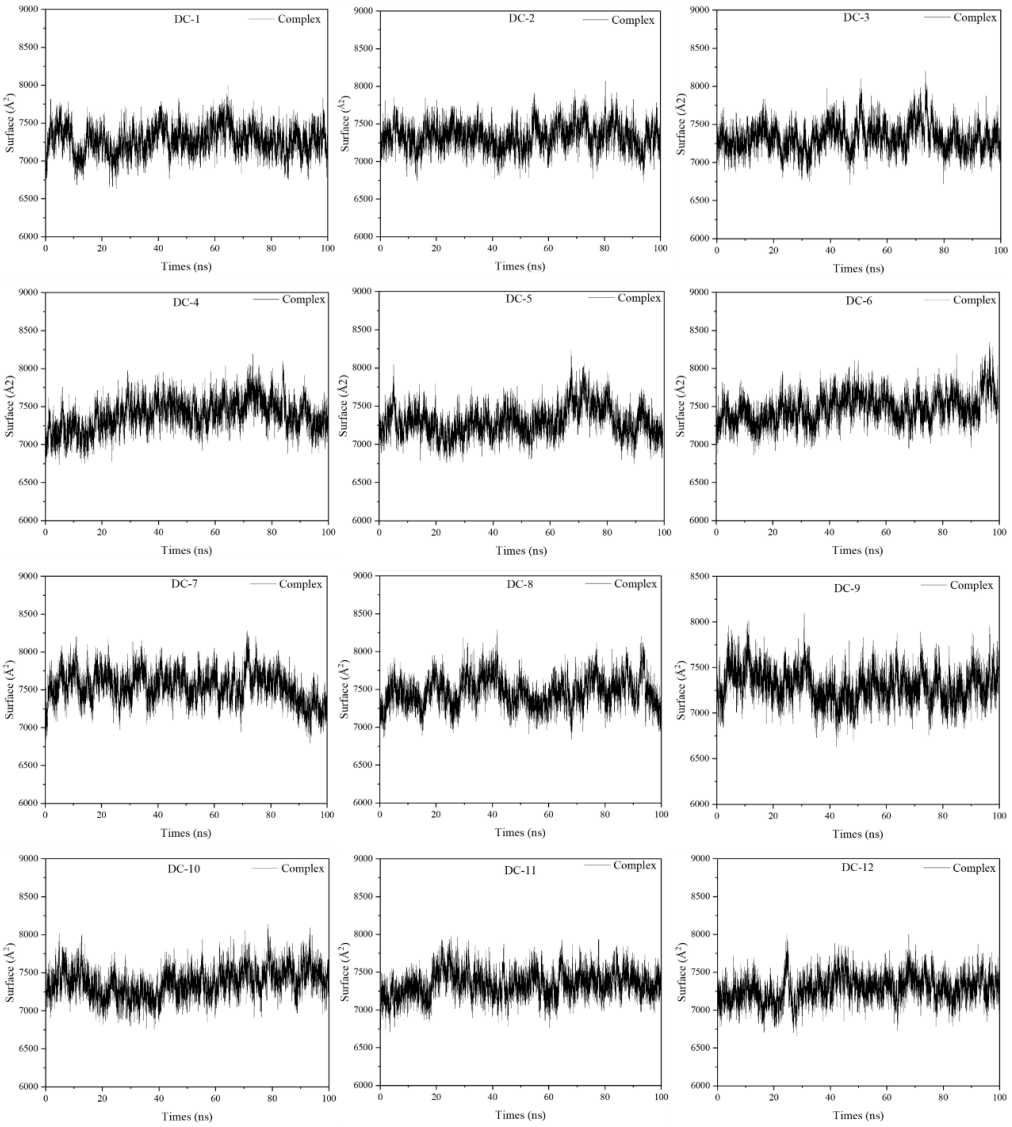

Figure S48. The surface areas of designed compounds with BRD4-BD1.

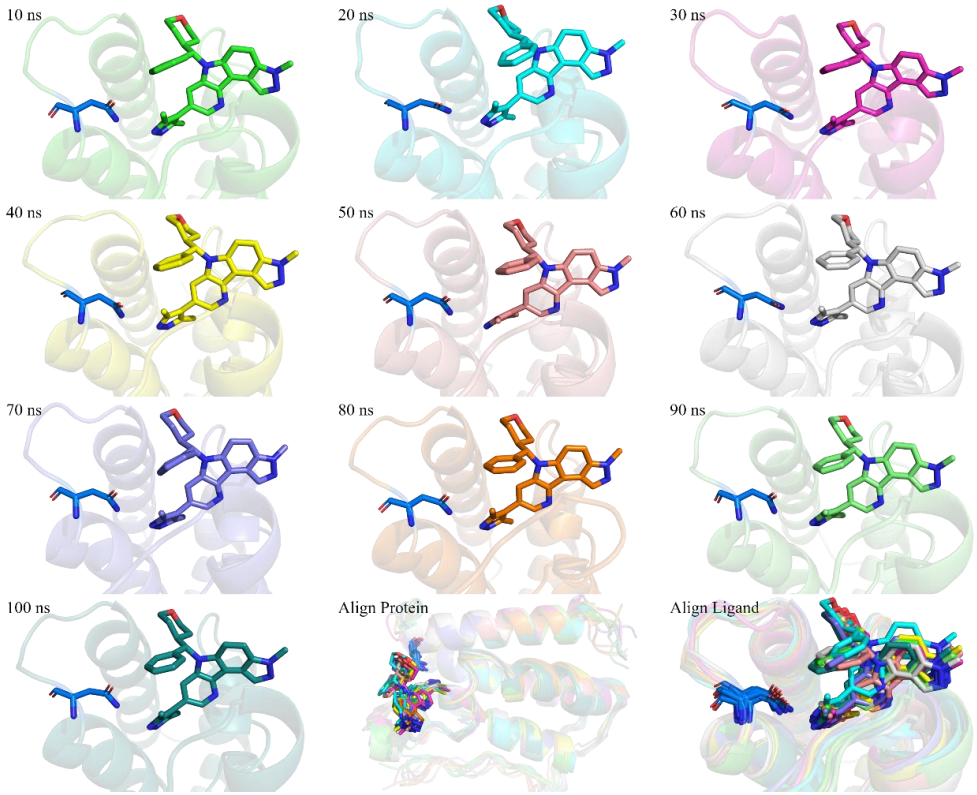

Figure S49. Snapshots of the DC-1/BRD4-BD1 along the dynamic simulation time. For clarity, the water molecules have been removed. The novel compound is plotted using stick style, while cartoon style for BRD4-BD1.

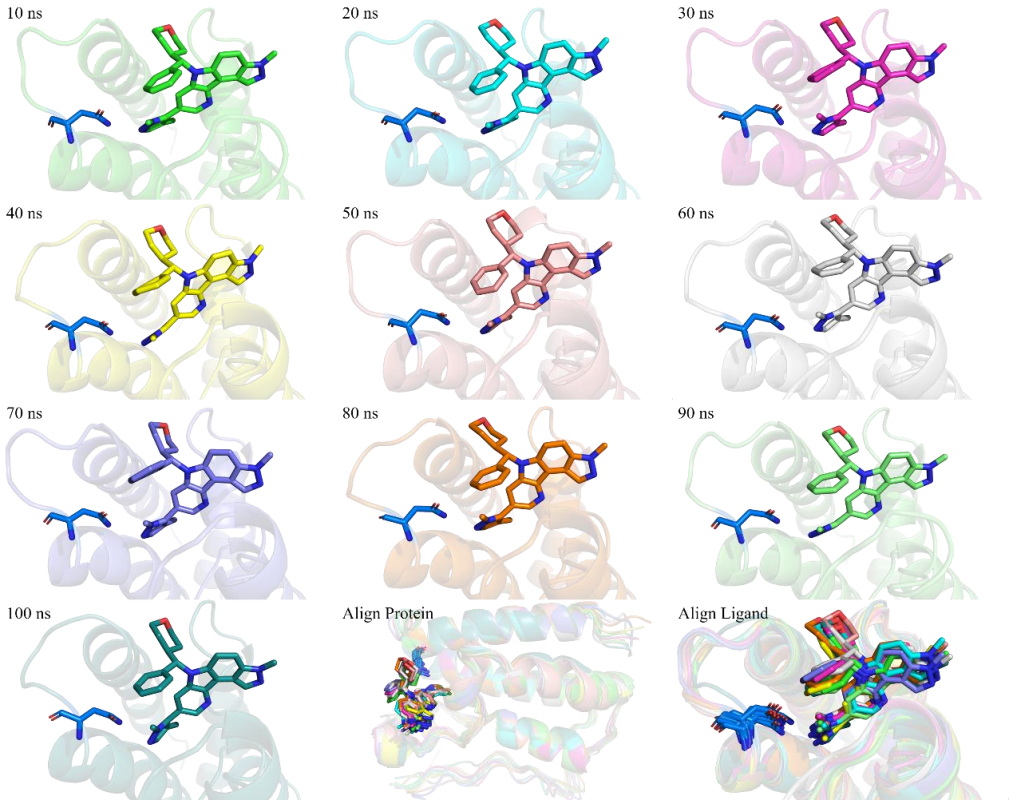

Figure S50. Snapshots of the DC-2/BRD4-BD1 along the dynamic simulation time. For clarity, the water molecules have been removed. The novel compound is plotted using stick style, while cartoon style for BRD4-BD1.

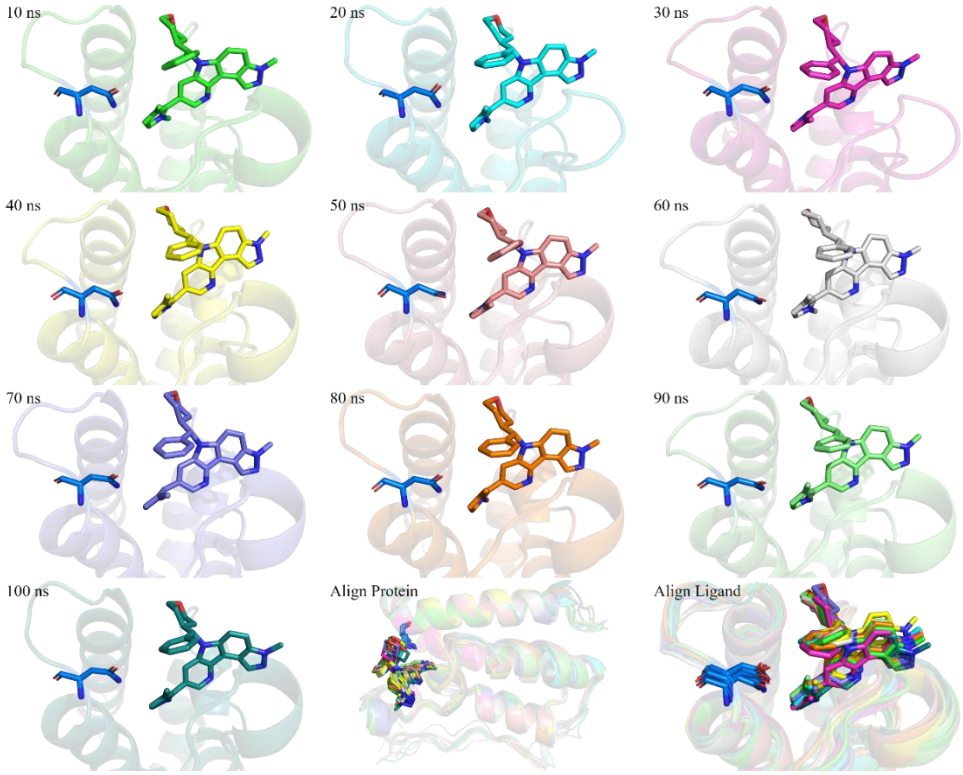

Figure S51. Snapshots of the DC-3/BRD4-BD1 along the dynamic simulation time. For clarity, the water molecules have been removed. The novel compound is plotted using stick style, while cartoon style for BRD4-BD1.

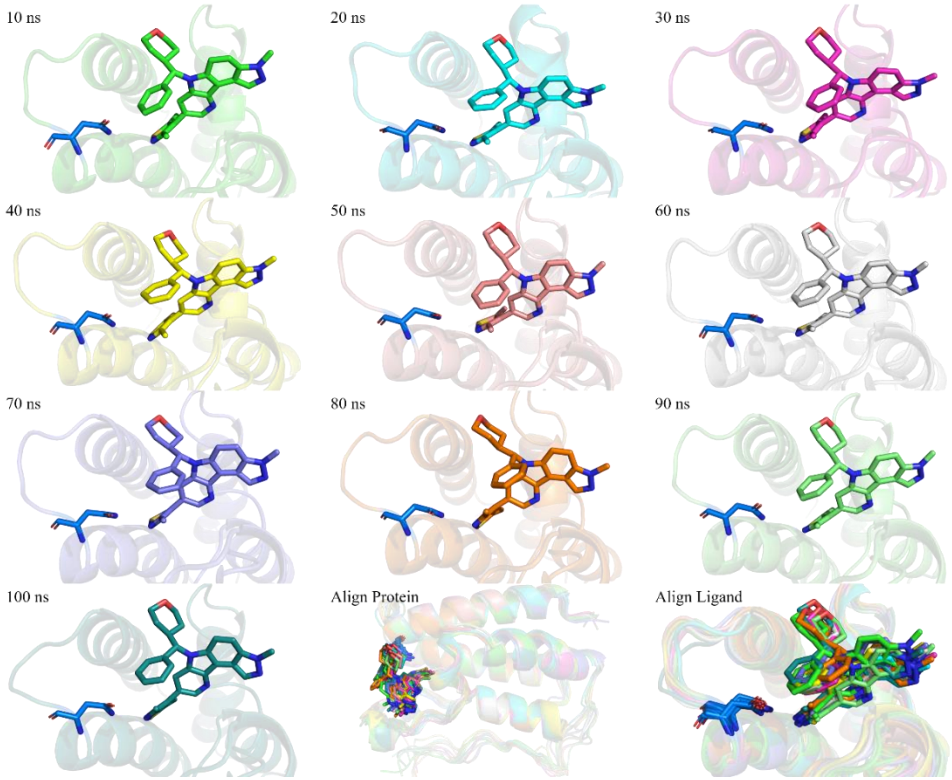

Figure S52. Snapshots of the DC-4/BRD4-BD1 along the dynamic simulation time. For clarity, the water molecules have been removed. The novel compound is plotted using stick style, while cartoon style for BRD4-BD1.

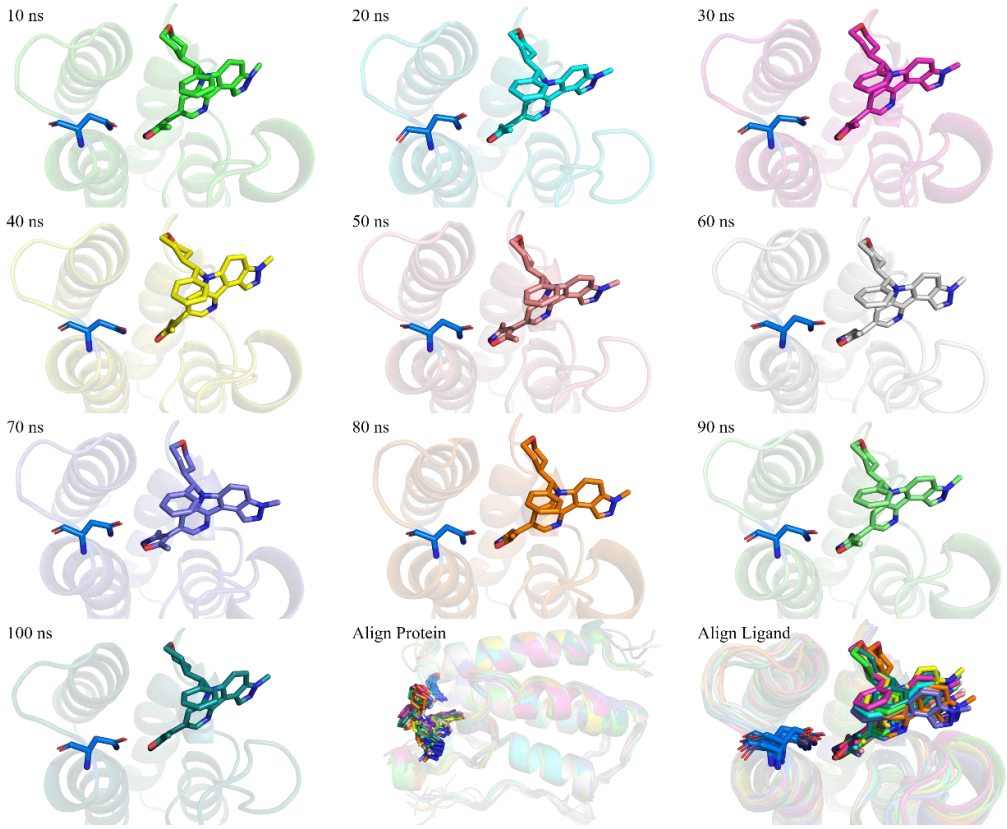

Figure S53. Snapshots of the DC-5/BRD4-BD1 along the dynamic simulation time. For clarity, the water molecules have been removed. The novel compound is plotted using stick style, while cartoon style for BRD4-BD1.

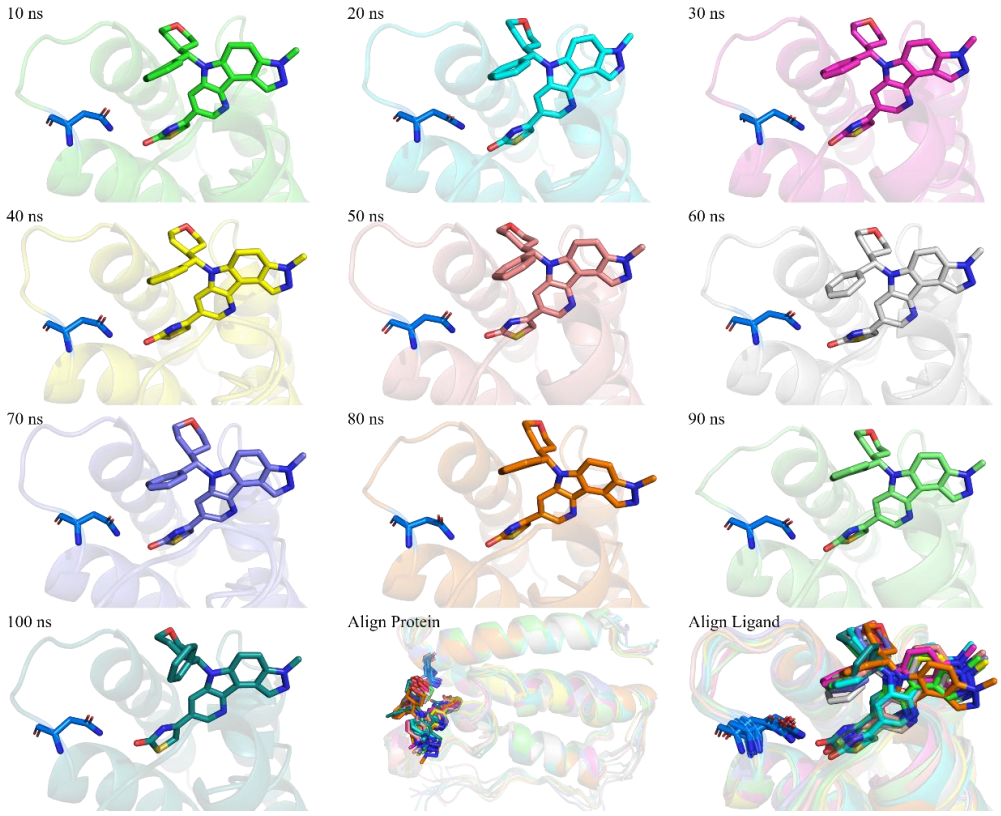

Figure S54. Snapshots of the DC-6/BRD4-BD1 along the dynamic simulation time. For clarity, the water molecules have been removed. The novel compound is plotted using stick style, while cartoon style for BRD4-BD1.

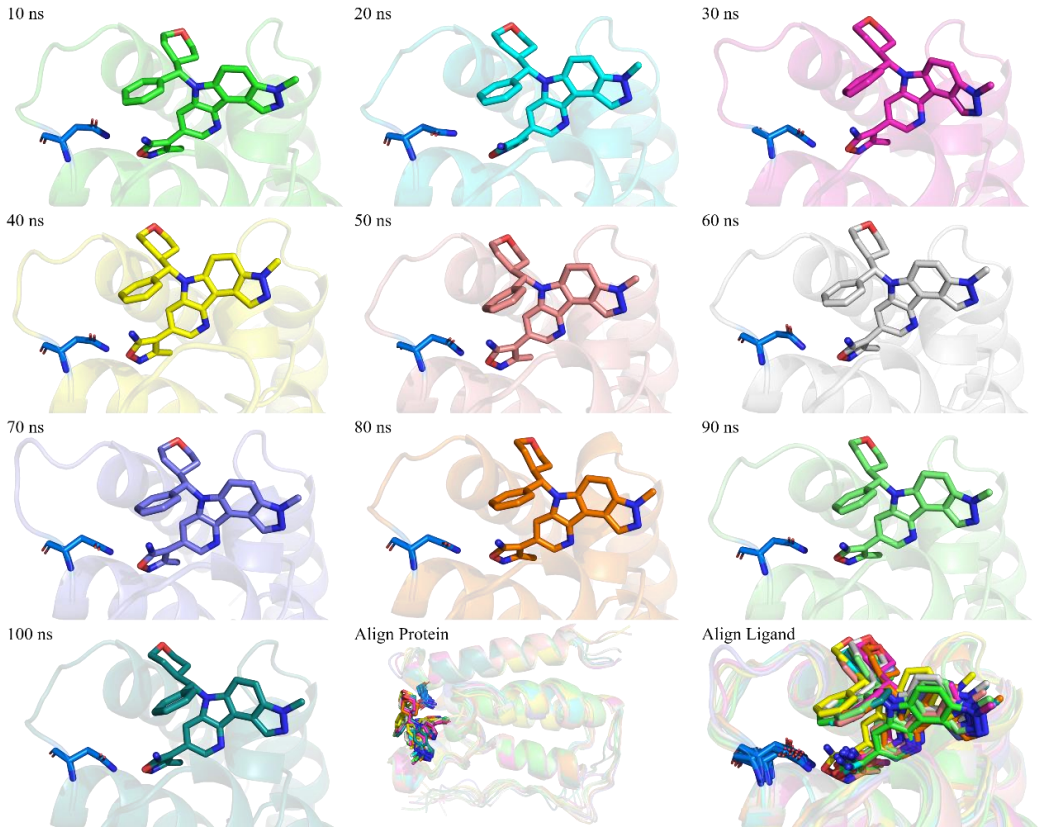

Figure S55. Snapshots of the DC-7/BRD4-BD1 along the dynamic simulation time. For clarity, the water molecules have been removed. The novel compound is plotted using stick style, while cartoon style for BRD4-BD1.

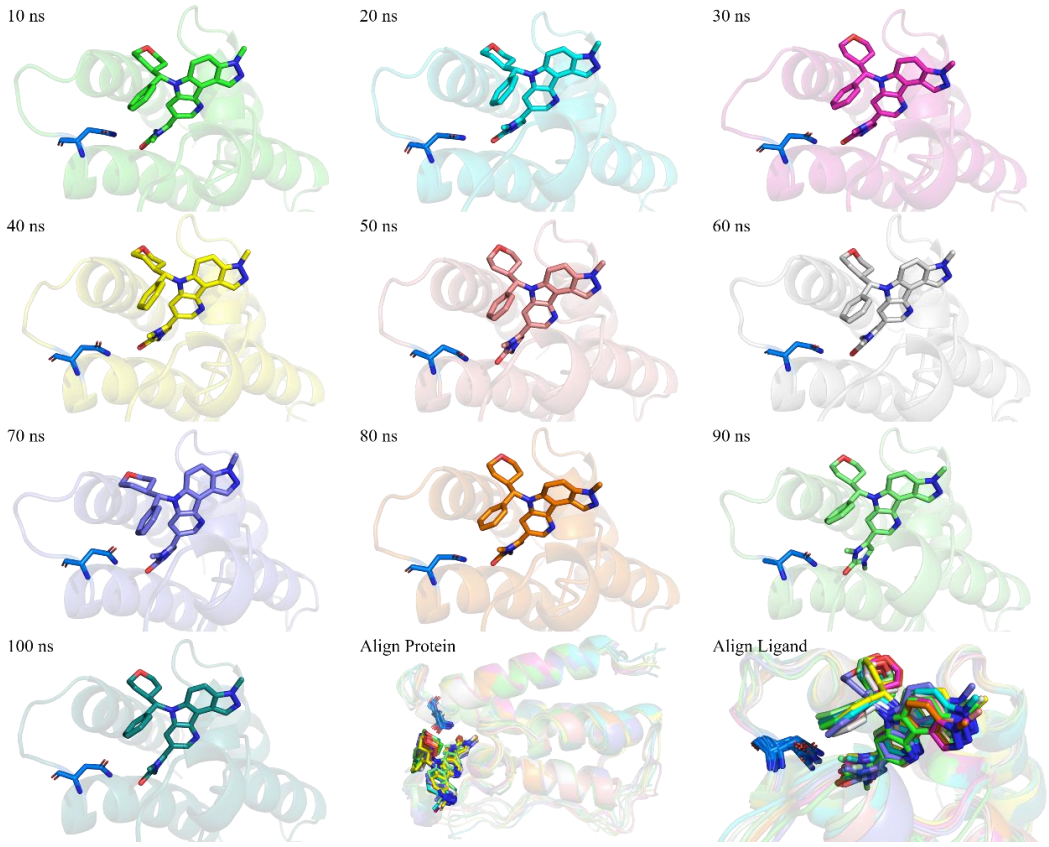

Figure S56. Snapshots of the DC-8/BRD4-BD1 along the dynamic simulation time. For clarity, the water molecules have been removed. The novel compound is plotted using stick style, while cartoon style for BRD4-BD1.

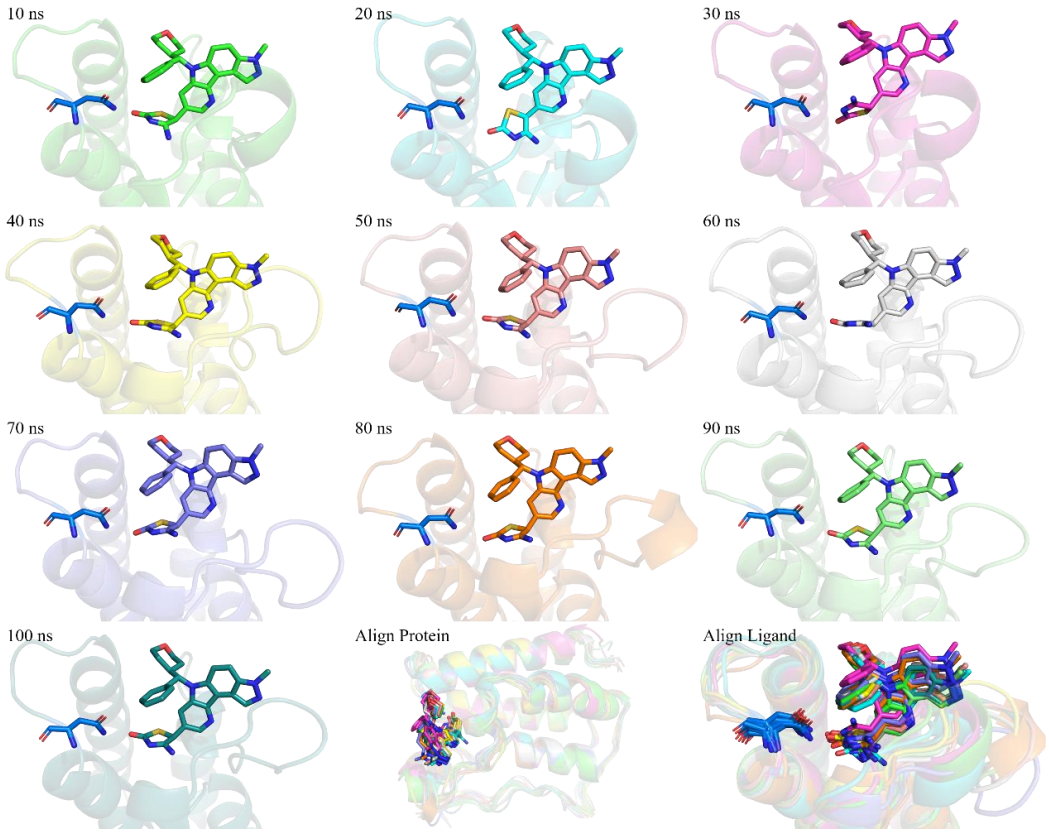

Figure S57. Snapshots of the DC-9/BRD4-BD1 along the dynamic simulation time. For clarity, the water molecules have been removed. The novel compound is plotted using stick style, while cartoon style for BRD4-BD1.

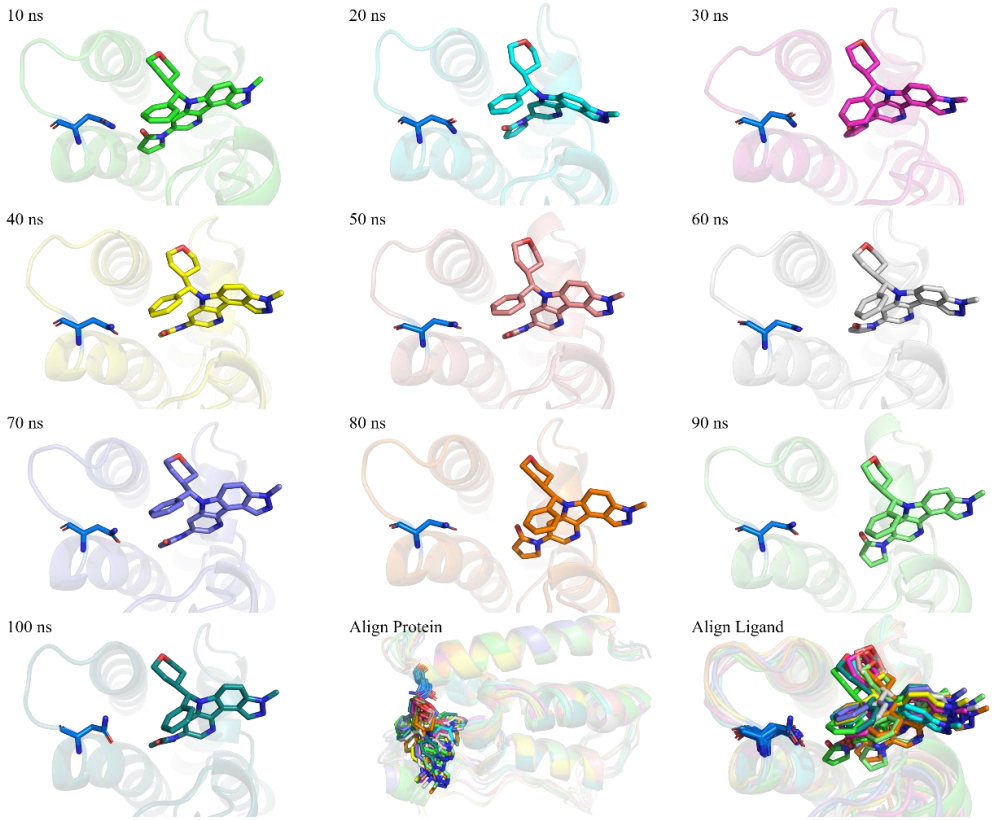

Figure S58. Snapshots of the DC-10/BRD4-BD1 along the dynamic simulation time. For clarity, the water molecules have been removed. The novel compound is plotted using stick style, while cartoon style for BRD4-BD1.

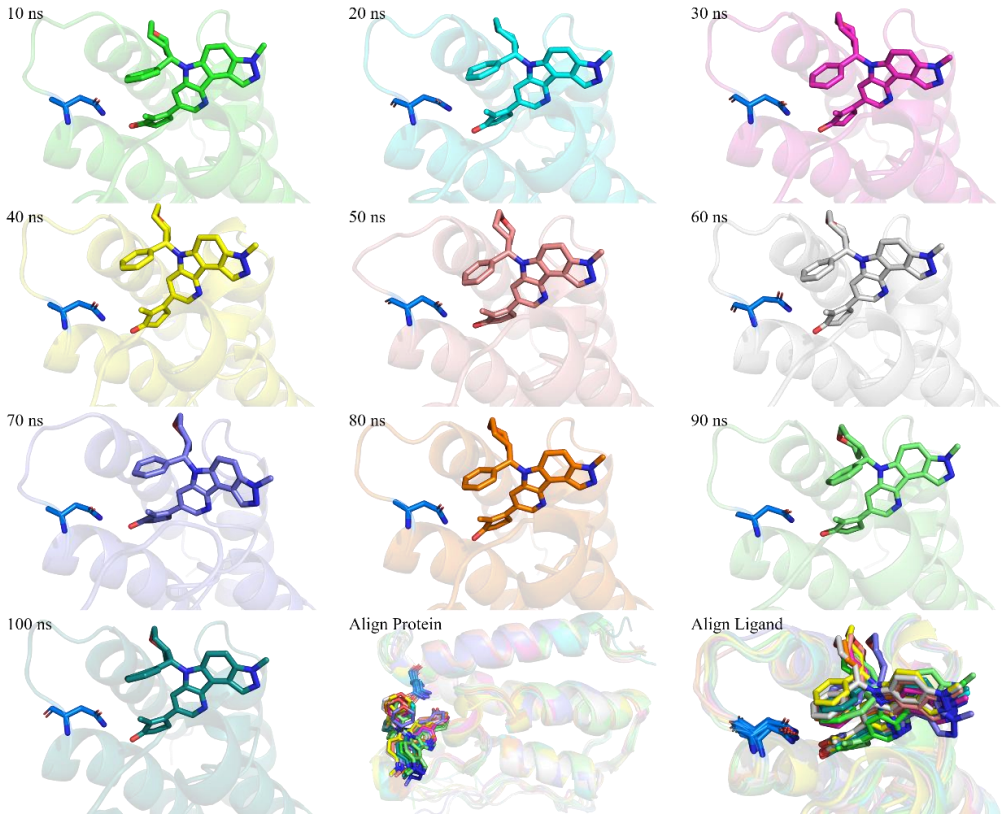

Figure S59. Snapshots of the DC-11/BRD4-BD1 along the dynamic simulation time. For clarity, the water molecules have been removed. The novel compound is plotted using stick style, while cartoon style for BRD4-BD1.

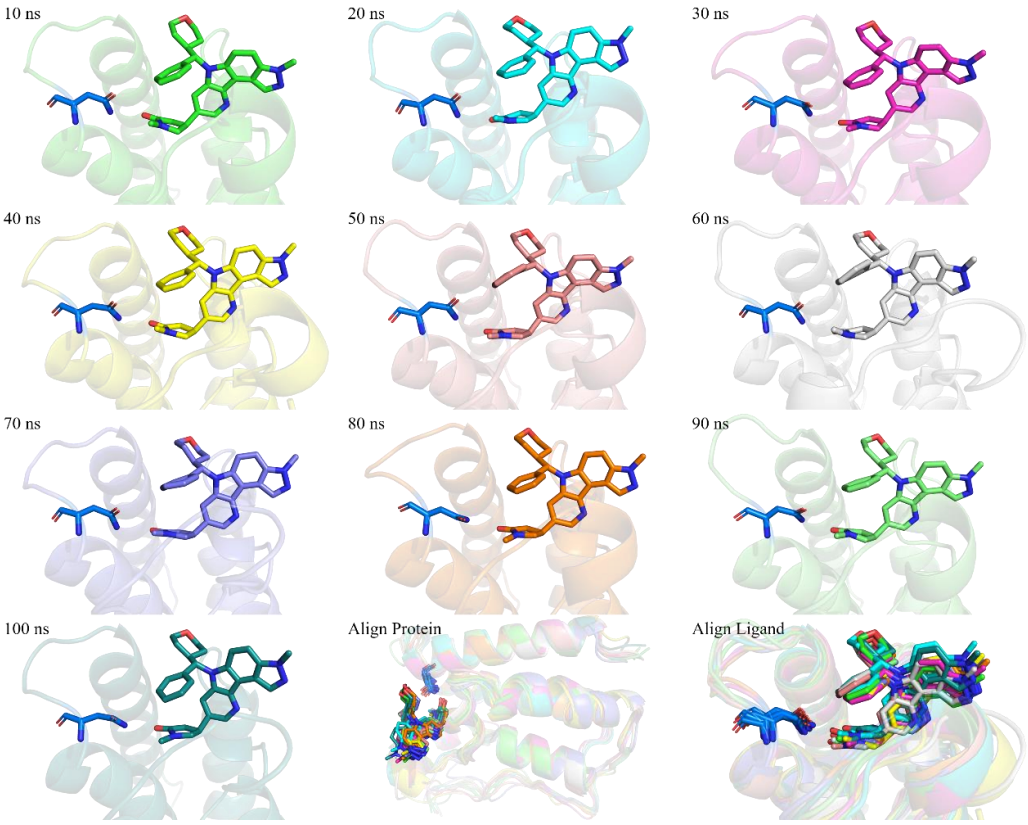

Figure S60. Snapshots of the DC-12/BRD4-BD1 along the dynamic simulation time. For clarity, the water molecules have been removed. The novel compound is plotted using stick style, while cartoon style for BRD4-BD1.

Table S1. The average root mean-squared fluctuation (RMSF) value for the BRD4-BD1 and BD2.

	BRD4-BD1		BRD4-BD2	
Lable	Average RMSF	Residue	Average RMSF	Residue
αZ	0.53 ± 0.10	61-76	0.70 ± 0.24	351-365
ZA loop	0.84 ± 0.17	77-106	0.63 ± 0.16	366-399
αA	0.54 ± 0.11	107-116	0.47 ± 0.12	400-409
AB loop	0.66 ± 0.10	117-121	0.68 ± 0.07	410-415
αB	0.51 ± 0.05	122-139	0.40 ± 0.07	416-432
BC loop	1.03 ± 0.37	140-144	0.60 ± 0.13	433-437
αC	0.63 ± 0.27	145-165	0.49 ± 0.12	438-456

The root mean-squared fluctuation (RMSF) values of the Cα atom of the residues in the bromodomain-containing protein 4 (BRD4) protein were measured among the 1000 ns molecular dynamics simulations for the NHWD-870 binding with BRD4-BD1 or BRD4-BD2. The average RMSF was calculated for αZ, ZA loop, αA, AB loop, αB, BC loop, and αC from the residues which listed in the table. The value was shown with average ± standard deviation. The residue number is according with human BRD4 protein sequence (UniProt ID: O60885).

Table S2. Hydrogen bonds network analysis for interactions between NHWD-870 (N87) and BRD4-BD1 (N140 and W81) and BD2 (N433 and W374).

Acceptor	Donor	Occupancy (%)	Average Distance (Å)	Average Angle (°)
N87@N2	N140@ND2	97.31	3.10 ± 0.17	160.78 ± 10.17
N87@N1	N140@ND2	40.55	3.58 ± 0.27	145.93 ± 11.06
N87@N2	N433@ND2	95.12	3.15 ± 0.19	161.07 ± 9.90
N87@N1	N433@ND2	50.34	3.51 ± 0.26	144.77 ± 10.59
N87@N6	W81@NE1	24.49	5.35 ± 2.13	82.07 ± 50.66
N87@N7	W81@NE1	10.16	5.38 ± 1.92	88.72 ± 50.40
N87@N6	W374@NE1	2.86	7.74 ± 1.64	44.02 ± 32.21
N87@N7	W374@NE1	1.52	7.61 ± 1.50	51.19 ± 31.12

Occupancy is in unit of percentage of the investigated time period (1000 ns), during which specific hydrogen bonds are formed. The hydrogen bond is defined as the distance of acceptor and donor atoms shorter than 3.5 Å, and the internal angle of acceptor···H-donor is larger than 120º.

* Standard deviation

Table S3. Binding free energy for NHWD-870/BRD4-BD1 complexes and decomposition to electrostatic interaction, van der Walls interaction, solvation free energies, and entropy.

Energy (kcal/mol)	Complex		Receptor		Ligand		Delta	
	Average	Std. Dev.*	Average	Std. Dev.	Average	Std. Dev.	Average	Std. Dev.
E_{vdW}	-1048.91	14.85	-993.68	14.72	-10.31	1.38	-44.93	2.94
E_{ele}	-9135.65	78.35	-9119.60	78.70	-1.15	0.91	-14.90	4.21
E_{GB}	-1712.28	66.84	-1718.97	67.17	-19.53	0.49	26.23	3.73
E_{surf}	53.20	1.29	54.42	1.27	4.07	0.04	-5.30	0.27
G_{gas}	-1992.51	78.37	-1961.61	78.26	28.92	5.69	-59.83	5.03
G_{solv}	-1659.09	66.31	-1664.55	66.65	-15.46	0.48	20.92	3.64
$E_{gas} + G_{sol}$	-3651.60	35.16	-3626.16	34.68	13.46	5.71	-38.90	2.72
TS_{total}	1513.96	6.37	1474.48	6.17	62.12	0.00	-22.64	4.41
ΔG_{bind}^{cal}							-16.27	5.18

* Standard deviation

Table S4. Binding free energy for NHWD-870/BRD4-BD2 complexes and decomposition to electrostatic interaction, van der Walls interaction, solvation free energies, and entropy.

Energy (kcal/mol)	Complex		Receptor		Ligand		Delta	
	Average	Std. Dev.*	Average	Std. Dev.	Average	Std. Dev.	Average	Std. Dev.
E_{vdW}	-897.50	12.97	-841.26	12.76	-9.58	1.56	-46.66	3.08
E_{ele}	-7987.16	84.98	-7969.71	84.48	-1.99	0.78	-15.46	3.75
E_{GB}	-1747.45	73.50	-1754.65	72.88	-19.21	0.42	26.41	3.56
E_{surf}	46.95	1.11	48.54	1.10	4.02	0.04	-5.62	0.28
G_{gas}	-1279.53	83.02	-1250.78	81.87	33.36	5.61	-62.11	5.15
G_{solv}	-1700.50	72.99	-1706.11	72.40	-15.19	0.41	20.80	3.41
$E_{gas} + G_{sol}$	-2980.04	32.47	-2956.89	31.75	18.17	5.62	-41.31	2.97
TS_{total}	1300.33	5.80	1263.14	5.86	61.72	0.00	-24.54	2.77
ΔG_{bind}^{cal}							-16.78	4.06

* Standard deviation

Table S5. Binding free energy for NHWD-870/BRD4-BD1 complexes and decomposition to electrostatic interaction, van der Walls interaction, solvation free energies, and entropy from the replica simulation.

Energy (kcal/mol)	Complex		Receptor		Ligand		Delta	
	Average	Std. Dev.*	Average	Std. Dev.	Average	Std. Dev.	Average	Std. Dev.
E_{vdW}	-1067.44	15.43	-1011.47	15.17	-10.21	1.33	-45.76	2.66
E_{ele}	-9130.18	81.95	-9117.44	82.17	-1.00	0.96	-11.73	3.81
E_{GB}	-1694.21	72.61	-1698.58	72.85	-19.52	0.47	23.89	3.63
E_{surf}	51.79	1.33	53.17	1.30	4.08	0.04	-5.46	0.24
G_{gas}	-2000.52	83.33	-1972.22	83.42	29.20	5.63	-57.50	4.58
G_{solv}	-1642.42	72.04	-1645.41	72.31	-15.44	0.45	18.43	3.54
$E_{gas} + G_{sol}$	-3642.94	36.57	-3617.63	36.20	13.75	5.64	-39.07	2.51
TS_{total}	1513.50	5.84	1473.50	7.23	62.12	0.00	-22.12	4.94
ΔG_{bind}^{cal}							-16.95	5.54

* Standard deviation

Table S6. Binding free energy for NHWD-870/BRD4-BD2 complexes and decomposition to electrostatic interaction, van der Walls interaction, solvation free energies, and entropy from the replica simulation.

Energy (kcal/mol)	Complex		Receptor		Ligand		Delta	
	Average	Std. Dev.*	Average	Std. Dev.	Average	Std. Dev.	Average	Std. Dev.
E_{vdW}	-896.68	13.22	-840.29	12.56	-9.56	1.65	-46.83	2.99
E_{ele}	-8000.96	84.06	-7982.99	83.92	-1.95	0.84	-16.02	3.90
E_{GB}	-1722.86	71.62	-1730.61	71.16	-19.23	0.42	26.97	3.52
E_{surf}	46.37	1.13	47.98	1.07	4.02	0.04	-5.63	0.29
G_{gas}	-1307.74	81.25	-1278.64	80.58	33.75	5.57	-62.85	4.96
G_{solv}	-1676.49	71.12	-1682.63	70.74	-15.20	0.41	21.34	3.40
$E_{gas} + G_{sol}$	-2984.23	31.21	-2961.27	30.62	18.54	5.58	-41.51	2.92
TS_{total}	1299.01	5.45	61.72	0.00	0.20	3.05	-24.16	3.05
ΔG_{bind}^{cal}							-17.35	4.22

* Standard deviation

Table S7. Free energy decomposition for the NHWD-870/BRD4-BD1 complex at the level of individual residues basis into contributions from van der Waals energy, electrostatic interaction energy, nonpolar solvation free energy, polar solvation free energy, or from backbone energy and side chain energy.

Residues	ΔE_{vdW}	ΔE_{ele}	$\Delta G_{sol,GB}$	$\Delta G_{sol,np}$	$\Delta G_{subtotal}$	$S\Delta G_{subtotal}$	$B\Delta G_{subtotal}$
W81	-1.77	-0.41	1.01	-0.33	-1.51	-1.21	-0.30
P82	-3.00	0.28	0.76	-0.32	-2.28	-2.02	-0.26
F83	-1.06	-0.04	0.22	-0.07	-0.94	-0.82	-0.13
Q85	-0.59	-0.21	0.50	-0.09	-0.40	-0.46	0.06
V87	-1.26	-0.18	0.26	-0.18	-1.37	-1.25	-0.12
K91	-0.37	-0.62	1.09	-0.08	0.02	-0.01	0.03
L92	-3.10	-0.62	1.14	-0.58	-3.15	-3.15	0.00
L94	-1.04	0.07	0.04	-0.21	-1.13	-1.16	0.03
Y97	-0.65	-0.66	0.80	-0.06	-0.57	-0.58	0.01
K102	0.00	-0.51	0.53	0.00	0.02	-0.01	0.02
D106	-0.05	1.02	-1.02	0.00	-0.05	-0.02	-0.03
K112	0.00	-0.52	0.53	0.00	0.01	0.01	0.01
R113	0.00	-0.55	0.56	0.00	0.01	0.00	0.01
D128	0.00	0.68	-0.68	0.00	-0.01	0.01	-0.01
C136	-0.86	-0.62	0.37	-0.07	-1.19	-0.71	-0.48
Y139	-0.76	-0.57	0.81	-0.04	-0.56	-0.55	-0.01
N140	-0.75	-3.34	2.85	-0.14	-1.38	-1.43	0.05
K141	-0.05	0.58	-0.49	0.00	0.04	0.01	0.03
D144	-0.22	-1.22	1.62	-0.02	0.15	0.21	-0.06
D145	-0.70	-0.49	1.07	-0.14	-0.26	-0.10	-0.16
I146	-3.52	0.47	-0.13	-0.35	-3.53	-3.33	-0.20
M149	-0.67	-0.11	0.29	-0.11	-0.60	-0.59	-0.02
E154	-0.01	0.60	-0.58	0.00	0.02	0.02	0.00

Energies are in kcal/mol.

Table S8. Free energy decomposition for the NHWD-870/BRD4-BD2 complex at the level of individual residues basis into contributions from van der Waals energy, electrostatic interaction energy, nonpolar solvation free energy, polar solvation free energy, or from backbone energy and side chain energy.

Residues	ΔE_{vdW}	ΔE_{ele}	$\Delta G_{sol,GB}$	$\Delta G_{sol,np}$	$\Delta G_{subtotal}$	$S\Delta G_{subtotal}$	$B\Delta G_{subtotal}$
W374	-2.73	0.22	0.87	-0.52	-2.17	-1.88	-0.30
P375	-2.63	0.33	0.64	-0.28	-1.94	-1.74	-0.21
F376	-0.90	-0.06	0.27	-0.07	-0.75	-0.68	-0.07
K378	-0.38	-1.96	2.41	-0.11	-0.03	-0.12	0.08
V380	-1.73	-0.19	0.30	-0.24	-1.87	-1.69	-0.17
L385	-2.75	-0.29	0.60	-0.52	-2.96	-2.94	-0.01
L387	-0.87	0.11	-0.01	-0.16	-0.94	-0.94	0.01
Y390	-0.69	-0.68	0.81	-0.04	-0.60	-0.60	0.01
K395	-0.01	-0.53	0.55	0.00	0.02	0.00	0.02
D399	-0.05	1.09	-1.10	0.00	-0.05	-0.03	-0.03
K404	0.00	-0.47	0.48	0.00	0.01	0.00	0.01
K406	0.00	-0.58	0.59	0.00	0.01	0.01	0.00
D421	0.00	0.75	-0.74	0.00	0.00	0.01	-0.01
R423	-0.01	-0.47	0.47	0.00	0.00	-0.01	0.01
C429	-0.90	-0.58	0.33	-0.07	-1.23	-0.71	-0.52
K431	-0.03	-1.21	1.28	0.00	0.04	-0.02	0.06
Y432	-0.95	-0.76	1.03	-0.07	-0.76	-0.72	-0.04
N433	-0.97	-3.37	2.99	-0.15	-1.50	-1.51	0.01
H437	-1.26	0.38	0.43	-0.25	-0.70	-0.50	-0.21
E438	-0.81	-0.16	0.13	-0.10	-0.94	-0.43	-0.51
V439	-2.72	0.09	-0.10	-0.21	-2.95	-2.50	-0.45
M442	-0.68	-0.13	0.27	-0.06	-0.60	-0.54	-0.05
R444	-0.02	-0.64	0.70	0.00	0.04	0.01	0.03
E451	0.00	0.49	-0.48	0.00	0.01	0.01	0.00

Energies are in kcal/mol.

Table S9. Hydrogen bonds network analysis for interactions between NHWD-870-R (N87) and BRD4-BD1 (N140) and BD2 (N433).

Acceptor	Donor	Occupancy (%)	Average Distance (Å)	Average Angle (°)
N87@N2	N140@ND2	97.17	3.10 ± 0.17	147.13 ± 11.01
N87@N1	N140@ND2	60.61	3.44 ± 0.26	160.56 ± 10.24
N87@N2	N433@ND2	95.71	3.44 ± 0.28	147.73 ± 11.70
N87@N1	N433@ND2	61.67	3.13 ± 0.20	159.54 ± 11.21

Occupancy is in unit of percentage of the investigated time period (1000 ns), during which specific hydrogen bonds are formed. The hydrogen bond is defined as the distance of acceptor and donor atoms shorter than 3.5 Å, and the internal angle of acceptor···H-donor is larger than 120º.

Table S10. Binding free energy for NHWD-870-R/BRD4-BD1 complexes and decomposition to electrostatic interaction, van der Walls interaction, solvation free energies, and entropy.

Energy (kcal/mol)	Complex		Receptor		Ligand		Delta	
	Average	Std. Dev.*	Average	Std. Dev.	Average	Std. Dev.	Average	Std. Dev.
E_{vdW}	-1059.33	16.24	-1003.09	15.98	-10.43	1.25	-45.81	3.00
E_{ele}	-9156.19	82.68	-9139.85	81.91	-7.78	0.93	-8.57	4.86
E_{GB}	-1693.27	72.39	-1692.89	71.82	-20.05	0.44	19.67	4.17
E_{surf}	51.90	1.53	53.01	1.47	4.16	0.04	-5.27	0.27
G_{gas}	-2013.43	83.32	-1994.69	82.31	35.63	5.51	-54.36	5.76
G_{solv}	-1641.37	71.63	-1639.88	71.09	-15.89	0.44	14.40	4.10
$E_{gas} + G_{sol}$	-3654.80	33.81	-3634.57	33.36	19.74	5.51	-39.97	3.12
TS_{total}	1513.92	5.93	1474.30	6.33	62.68	0.12	-23.07	3.49
ΔG_{bind}^{cal}							-16.90	4.68

* Standard deviation

Table S11. Binding free energy for NHWD-870-R/BRD4-BD2 complexes and decomposition to electrostatic interaction, van der Walls interaction, solvation free energies, and entropy.

Energy (kcal/mol)	Complex		Receptor		Ligand		Delta	
	Average	Std. Dev.*	Average	Std. Dev.	Average	Std. Dev.	Average	Std. Dev.
E_{vdW}	-892.32	14.17	-836.87	13.59	-10.02	1.36	-45.43	3.46
E_{ele}	-7985.29	85.34	-7961.23	85.48	-7.68	0.86	-16.39	3.32
E_{GB}	-1721.71	72.27	-1728.36	72.48	-20.02	0.44	26.67	2.98
E_{surf}	46.94	1.30	48.19	1.24	4.14	0.05	-5.40	0.32
G_{gas}	-1299.21	85.21	-1273.91	84.90	36.52	5.66	-61.82	4.81
G_{solv}	-1674.77	71.63	-1680.16	71.88	-15.88	0.44	21.28	2.85
$E_{gas} + G_{sol}$	-2973.98	33.43	-2954.07	32.68	20.63	5.67	-40.54	3.45
TS_{total}	1302.25	6.53	1263.82	6.82	62.68	0.05	-24.25	3.26
ΔG_{bind}^{cal}							-16.29	4.75

* Standard deviation

Table S12. Binding free energy for compound DC-1/BRD4-BD1 complex and decomposition to electrostatic interaction, van der Walls interaction, solvation free energies, and entropy.

Energy(kcal/mol)	Complex		Receptor		Ligand		Delta	
	Average	Std. Dev.*	Average	Std. Dev.	Average	Std. Dev.	Average	Std. Dev.
E_{vdW}	-1057.38	14.46	-999.05	14.32	-9.95	1.44	-48.38	2.52
E_{ele}	-9176.30	75.48	-9185.71	75.01	25.10	1.03	-15.69	5.60
E_{GB}	-1661.84	63.31	-1669.04	63.40	-23.09	0.52	30.30	4.88
E_{surf}	52.21	1.20	53.88	1.19	4.07	0.03	-5.74	0.26
G_{gas}	-2051.69	77.86	-2014.00	77.52	26.37	5.44	-64.07	6.36
G_{solv}	-1609.63	62.74	-1615.16	62.83	-19.02	0.51	24.56	4.72
$E_{gas} + G_{sol}$	-3661.32	36.00	-3629.16	35.30	7.35	5.44	-39.51	2.90
TS_{total}	1510.27	6.40	1472.09	6.84	62.78	0.00	-24.59	5.33
ΔG_{bind}^{cal}							-14.91	6.07

* Standard deviation

Table S13. Binding free energy for compound DC-2/BRD4-BD1 complex and decomposition to electrostatic interaction, van der Walls interaction, solvation free energies, and entropy.

Energy(kcal/mol)	Complex		Receptor		Ligand		Delta	
	Average	Std. Dev.*	Average	Std. Dev.	Average	Std. Dev.	Average	Std. Dev.
E_{vdW}	-1051.73	14.86	-995.16	14.62	-10.18	1.31	-46.38	2.63
E_{ele}	-9118.36	78.84	-9124.11	78.36	19.61	0.93	-13.86	4.28
E_{GB}	-1703.08	66.92	-1709.32	66.28	-20.77	0.52	27.01	4.10
E_{surf}	52.73	1.39	54.14	1.32	4.12	0.04	-5.54	0.26
G_{gas}	-1985.55	78.92	-1968.05	77.88	42.74	5.34	-60.23	5.32
G_{solv}	-1650.36	66.25	-1655.18	65.67	-16.65	0.50	21.47	3.97
$E_{gas} + G_{sol}$	-3635.91	35.53	-3623.23	35.11	26.08	5.36	-38.76	2.65
TS_{total}	1514.03	5.87	1474.74	6.43	62.10	0.00	-22.82	4.67
ΔG_{bind}^{cal}							-15.94	5.37

* Standard deviation

Table S14. Binding free energy for compound DC-3/BRD4-BD1 complex and decomposition to electrostatic interaction, van der Walls interaction, solvation free energies, and entropy.

Energy(kcal/mol)	Complex		Receptor		Ligand		Delta	
	Average	Std. Dev.*	Average	Std. Dev.	Average	Std. Dev.	Average	Std. Dev.
E_{vdW}	-1052.86	14.30	-996.17	14.08	-10.41	1.30	-46.28	2.71
E_{ele}	-9145.55	68.42	-9154.85	67.99	22.16	0.92	-12.86	3.88
E_{GB}	-1678.86	62.00	-1686.81	61.85	-18.47	0.44	26.43	3.39
E_{surf}	52.32	1.10	53.57	1.08	4.17	0.04	-5.42	0.23
G_{gas}	-2023.37	71.60	-2002.60	71.08	38.37	5.56	-59.14	4.67
G_{solv}	-1626.54	61.46	-1633.24	61.30	-14.30	0.42	21.00	3.29
$E_{gas} + G_{sol}$	-3649.91	36.00	-3635.84	35.30	24.07	5.56	-38.13	2.61
TS_{total}	1514.83	5.79	1475.65	5.56	62.47	0.00	-23.29	4.72
ΔG_{bind}^{cal}							-14.85	5.39

* Standard deviation

Table S15. Binding free energy for compound DC-4/BRD4-BD1 complex and decomposition to electrostatic interaction, van der Walls interaction, solvation free energies, and entropy.

Energy(kcal/mol)	Complex		Receptor		Ligand		Delta	
	Average	Std. Dev.*	Average	Std. Dev.	Average	Std. Dev.	Average	Std. Dev.
E_{vdW}	-1052.64	14.22	-995.69	13.93	-9.98	1.50	-46.97	2.57
E_{ele}	-9055.69	79.90	-9069.45	80.10	24.67	0.97	-10.91	3.74
E_{GB}	-1753.57	67.95	-1758.57	68.35	-18.60	0.43	23.59	3.51
E_{surf}	53.10	1.36	54.51	1.35	4.19	0.03	-5.60	0.25
G_{gas}	-1947.57	77.99	-1920.05	78.35	30.36	5.52	-57.88	4.54
G_{solv}	-1700.47	67.32	-1704.05	67.69	-14.41	0.42	18.00	3.40
$E_{gas} + G_{sol}$	-3648.04	34.39	-3624.11	34.04	15.95	5.52	-39.88	2.53
TS_{total}	1515.81	5.64	1475.39	6.68	63.43	0.00	-23.01	4.71
ΔG_{bind}^{cal}							-16.88	5.35

* Standard deviation

Table S16. Binding free energy for compound DC-5/BRD4-BD1 complex and decomposition to electrostatic interaction, van der Walls interaction, solvation free energies, and entropy.

Energy(kcal/mol)	Complex		Receptor		Ligand		Delta	
	Average	Std. Dev.*	Average	Std. Dev.	Average	Std. Dev.	Average	Std. Dev.
E_{vdW}	-1054.98	14.57	-999.55	14.31	-10.07	1.37	-45.36	2.60
E_{ele}	-9139.87	81.67	-9142.05	81.62	14.72	1.13	-12.54	3.82
E_{GB}	-1669.54	73.23	-1674.18	73.30	-20.95	0.53	25.59	3.63
E_{surf}	52.18	1.31	53.59	1.28	4.08	0.04	-5.49	0.25
G_{gas}	-2055.03	85.15	-2013.22	85.07	16.08	5.56	-57.89	4.67
G_{solv}	-1617.36	72.50	-1620.59	72.59	-16.87	0.52	20.10	3.56
$E_{gas} + G_{sol}$	-3672.39	34.14	-3633.80	33.66	-0.79	5.57	-37.80	2.51
TS_{total}	1514.87	6.63	1475.03	7.23	62.72	0.12	-22.88	9.81
ΔG_{bind}^{cal}							-14.91	5.31

* Standard deviation

Table S17. Binding free energy for compound DC-6/BRD4-BD1 complex and decomposition to electrostatic interaction, van der Walls interaction, solvation free energies, and entropy.

Energy(kcal/mol)	Complex		Receptor		Ligand		Delta	
	Average	Std. Dev.*	Average	Std. Dev.	Average	Std. Dev.	Average	Std. Dev.
E_{vdW}	-1039.34	14.93	-988.93	14.40	-9.02	1.07	-41.40	2.83
E_{ele}	-9009.46	91.11	-9038.94	91.27	47.96	1.09	-18.49	4.58
E_{GB}	-1774.93	92.51	-1780.59	92.54	-23.55	0.60	29.20	4.14
E_{surf}	54.61	1.50	55.58	1.45	4.24	0.03	-5.21	0.26
G_{gas}	-1919.69	104.97	-1889.76	104.58	29.94	5.47	-59.87	5.42
G_{solv}	-1720.33	91.50	-1725.01	91.57	-19.30	0.59	23.99	4.00
$E_{gas} + G_{sol}$	-3640.01	35.43	-3614.77	34.98	10.64	5.44	-35.88	2.68
TS_{total}	1518.43	7.14	1479.95	6.17	60.04	0.00	-21.56	4.21
ΔG_{bind}^{cal}							-14.32	4.99

* Standard deviation

Table S18. Binding free energy for compound DC-7/BRD4-BD1 complex and decomposition to electrostatic interaction, van der Walls interaction, solvation free energies, and entropy.

Energy(kcal/mol)	Complex		Receptor		Ligand		Delta	
	Average	Std. Dev.*	Average	Std. Dev.*	Average	Std. Dev.*	Average	Std. Dev.*
E_{vdW}	-1039.72	14.08	-988.96	13.96	-9.82	1.34	-40.95	2.43
E_{ele}	-9120.48	83.31	-9111.84	83.73	11.24	1.36	-19.87	4.69
E_{GB}	-1707.36	83.22	-1714.99	83.78	-24.90	0.82	32.53	4.04
E_{surf}	53.28	1.46	54.33	1.44	4.06	0.04	-5.11	0.22
G_{gas}	-2021.62	96.53	-1968.46	96.60	7.66	5.72	-60.82	5.21
G_{solv}	-1654.08	82.41	-1660.66	82.98	-20.84	0.80	27.42	3.96
$E_{gas} + G_{sol}$	-3675.70	35.40	-3629.12	34.75	-13.19	5.74	-33.40	2.49
TS_{total}	1515.59	7.37	1474.96	7.68	62.19	0.01	-21.55	4.43
ΔG_{bind}^{cal}							-11.85	5.09

* Standard deviation

Table S19. Binding free energy for compound DC-8/BRD4-BD1 complex and decomposition to electrostatic interaction, van der Walls interaction, solvation free energies, and entropy.

Energy(kcal/mol)	Complex		Receptor		Ligand		Delta	
	Average	Std. Dev.*	Average	Std. Dev.	Average	Std. Dev.	Average	Std. Dev.
E_{vdW}	-1042.29	15.18	-985.19	14.69	-10.19	1.28	-46.91	3.18
E_{ele}	-9100.16	83.57	-9050.46	82.72	-25.61	1.24	-24.10	5.70
E_{GB}	-1770.40	74.76	-1779.11	73.81	-25.59	0.60	34.30	4.78
E_{surf}	54.03	1.49	55.42	1.43	4.30	0.04	-5.69	0.28
G_{gas}	-1856.61	86.61	-1896.39	85.13	110.78	5.52	-71.00	6.80
G_{solv}	-1716.37	73.94	-1723.69	73.04	-21.29	0.58	28.62	4.63
$E_{gas} + G_{sol}$	-3572.98	34.97	-3620.08	34.35	89.49	5.52	-42.39	3.52
TS_{total}	1518.86	6.06	1479.04	5.85	63.93	0.17	-24.11	8.43
ΔG_{bind}^{cal}							-18.28	5.34

* Standard deviation

Table S20. Binding free energy for compound DC-9/BRD4-BD1 complex and decomposition to electrostatic interaction, van der Walls interaction, solvation free energies, and entropy.

Energy(kcal/mol)	Complex		Receptor		Ligand		Delta	
	Average	Std. Dev.*	Average	Std. Dev.	Average	Std. Dev.	Average	Std. Dev.
E_{vdW}	-1055.89	15.05	-999.47	14.77	-10.01	1.16	-46.41	2.77
E_{ele}	-9038.16	73.98	-9138.40	73.33	115.69	1.73	-15.46	4.14
E_{GB}	-1713.68	65.94	-1717.43	65.32	-27.57	1.05	31.32	3.57
E_{surf}	52.42	1.29	54.14	1.29	4.18	0.05	-5.90	0.27
G_{gas}	-2099.70	74.88	-1957.14	74.51	-80.70	5.63	-61.86	4.78
G_{solv}	-1661.26	65.38	-1663.29	64.73	-23.39	1.03	25.42	3.50
$E_{gas} + G_{sol}$	-3760.97	34.83	-3620.44	34.17	-104.09	5.59	-36.44	2.95
TS_{total}	1516.01	5.54	1475.60	6.26	63.05	0.00	-22.64	4.74
ΔG_{bind}^{cal}							-13.80	5.58

* Standard deviation

Table S21. Binding free energy for compound DC-10/BRD4-BD1 complex and decomposition to electrostatic interaction, van der Walls interaction, solvation free energies, and entropy.

Energy(kcal/mol)	Complex		Receptor		Ligand		Delta	
	Average	Std. Dev.*	Average	Std. Dev.	Average	Std. Dev.	Average	Std. Dev.
E_{vdW}	-1042.05	14.92	-991.67	14.51	-8.38	1.44	-42.01	3.25
E_{ele}	-9076.25	73.92	-9097.59	74.82	33.46	1.40	-12.12	5.92
E_{GB}	-1741.43	63.24	-1744.84	63.72	-24.25	0.96	27.66	4.93
E_{surf}	53.81	1.19	54.61	1.19	4.10	0.04	-4.90	0.36
G_{gas}	-1939.78	75.05	-1927.65	75.58	42.00	5.47	-54.13	6.18
G_{solv}	-1687.63	62.75	-1690.23	63.16	-20.15	0.96	22.76	4.83
$E_{gas} + G_{sol}$	-3627.41	33.87	-3617.88	33.24	21.85	5.48	-31.37	3.02
TS_{total}	1513.60	6.01	1475.81	6.90	59.01	0.02	-21.21	4.53
ΔG_{bind}^{cal}							-10.16	5.44

* Standard deviation

Table S22. Binding free energy for compound DC-11/BRD4-BD1 complex and decomposition to electrostatic interaction, van der Walls interaction, solvation free energies, and entropy.

Energy(kcal/mol)	Complex		Receptor		Ligand		Delta	
	Average	Std. Dev.*	Average	Std. Dev.	Average	Std. Dev.	Average	Std. Dev.
E_{vdW}	-1047.96	14.09	-996.10	13.94	-9.56	1.45	-42.30	2.93
E_{ele}	-9205.78	73.72	-9161.15	73.66	-27.59	1.08	-17.03	4.44
E_{GB}	-1687.48	66.89	-1692.77	66.91	-22.13	0.54	27.42	3.89
E_{surf}	53.11	1.07	54.18	1.06	4.16	0.04	-5.23	0.28
G_{gas}	-1936.84	74.99	-1993.44	75.14	115.94	5.42	-59.33	5.46
G_{solv}	-1634.37	66.46	-1638.59	66.47	-17.97	0.52	22.19	3.74
$E_{gas} + G_{sol}$	-3571.21	32.67	-3632.03	32.44	97.97	5.40	-37.15	2.80
TS_{total}	1513.44	6.00	1475.65	5.15	61.11	0.00	-23.31	4.49
ΔG_{bind}^{cal}							-13.83	5.29

* Standard deviation

Table S23. Binding free energy for compound DC-12/BRD4-BD1 complex and decomposition to electrostatic interaction, van der Walls interaction, solvation free energies, and entropy.

Energy(kcal/mol)	Complex		Receptor		Ligand		Delta	
	Average	Std. Dev.*	Average	Std. Dev.	Average	Std. Dev.	Average	Std. Dev.
E_{vdW}	-1052.06	14.45	-996.56	14.20	-10.47	1.29	-45.03	3.25
E_{ele}	-9156.01	72.11	-9130.77	72.19	-7.45	1.22	-17.79	5.16
E_{GB}	-1694.87	67.14	-1700.68	66.89	-23.98	0.73	29.78	4.84
E_{surf}	52.63	1.14	53.94	1.15	4.12	0.07	-5.42	0.31
G_{gas}	-1969.22	77.43	-1978.69	77.16	72.29	5.59	-62.81	6.33
G_{solv}	-1642.24	66.75	-1646.75	66.49	-19.86	0.69	24.36	4.67
$E_{gas} + G_{sol}$	-3611.46	33.32	-3625.44	33.11	52.43	5.56	-38.45	3.03
TS_{total}	1514.44	6.01	1474.49	6.19	63.13	0.00	-23.18	3.96
ΔG_{bind}^{cal}							-15.28	4.99

* Standard deviation